Canada

CCAF Project A073

SUMMARY REPORT

Ground Thermal Modeling in Support of Terrain Evaluation and Route Selection in the Mackenzie River Valley

J.F. Wright, C. Duchesne, F. M. Nixon, M. Côté

Natural Resources Canada

Geological Survey of Canada

August, 2001

List of Figures

1 INTRODUCTION

In 1999, Canada's Climate Change Action Fund (CCAF) approved a 2-year research project (CCAF No. A073) authorized for FY's 1999-00 & 2000-01 to develop appropriate databases and ground thermal modeling capacity in support of terrain evaluation and route selection projects related to anticipated highway and pipeline development in the Mackenzie River Valley during the next decade. The project constitutes a significant component of GSC-TSD's permafrost modeling and mapping effort, which is supported through GSC A-base funding and through additional funding from the Program of Energy Research and Development (PERD). A summary of individual project tasks and their status at the time of writing of this report is available in Appendix 1.

1.1 Background

As a consequence of continued climate warming, ground temperatures are expected to increase throughout Canada during the next century. In permafrost terrain, warming of the ground will lead to a general increase in the thickness of the annual thaw (active) layer, and to partial or complete thawing of permafrost where ground temperatures are currently close to 0°C. Progressive thawing of frozen ground will have potentially serious implications for the stability of engineered structures, the reliability of transportation routes, and the viability of traditional hunting and fishing practices in Canada's permafrost regions. The physical expression of warmer ground temperatures will include more extensive ground subsidence, greater frequency of slope failure, and significant and occasionally catastrophic changes to surface and ground water flows.

Unfortunately, techniques for mapping the distribution and thickness of permafrost are generally poorly developed. The current map standard for permafrost in Canada simply delineates a number of broad zones within which the distribution of permafrost is considered to be either continuous, discontinuous, or sporadic (Hegginbottom et al., 1995). While useful for visualising the generalised distribution of permafrost from a continental perspective, such maps are inadequate for addressing climate change issues because they provide no information about the actual distribution of frozen vs. unfrozen ground, the existing range of ground temperatures, or local/regional variations in permafrost thickness.

A truly useful tool for investigating the climate-permafrost relations should describe explicit linkages between the major climate and terrain factors influencing the occurrence of permafrost, thereby facilitating prediction of expected changes to the ground thermal regime in response to a number of alternative climate scenarios. A simple conceptual model proposed by Luthin and Guymon (1974) incorporates the dominant climate and terrain factors influencing the ground thermal state and describes the primary linkages between the atmospheric and ground thermal regimes (Figure 1). This highly generalized scheme is compatible (with respect to model parameterisation) with the sophisticated finite-element model (T-ONE) and the simple numeric relation (TTOP) described in the following sections of this report.

Figure 1: A conceptual model of the climate-permafrost system

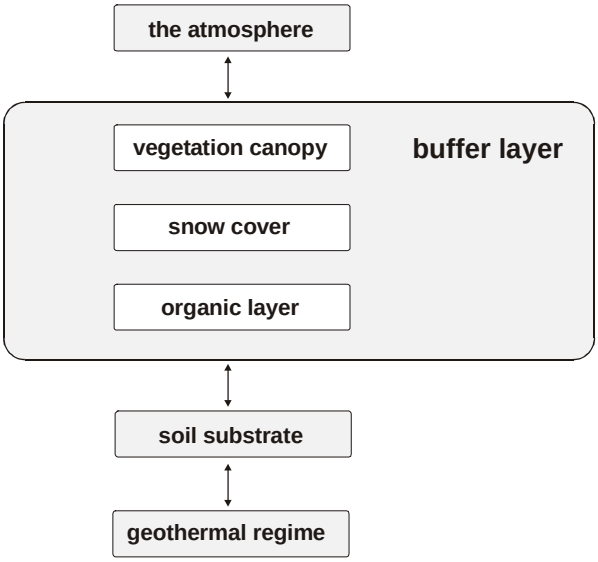

During the past 5 years the GSC has developed a physically based, regional-scale ground thermal modeling capability which utilizes a simple numeric relation compatible with the conceptual model described above to predict the occurrence and thickness of permafrost. Within this framework, the assignment of suitable model input parameters values is based on generalized descriptions of regional climate (Environment Canada climate normals) and local terrain conditions (available map data and satellite imagery). As a physical model, therefore, model outputs are directly linked to key properties and processes of climate and terrain (model inputs), facilitating the investigation of ground thermal responses to alternative climates. Calibration of the model and validation of its performance is supported by ground truth data from geotechnical borehole records and an extensive network of ground temperature monitoring sites established by the GSC in the Mackenzie Valley, NWT.

In this work, the GSC modeling framework was applied to the investigation of climate-induced impacts on permafrost within the greater Mackenzie River Valley. The initial focus of the study was on low-resolution (1km) modeling of potential changes to permafrost (in terms of distribution and thickness) within the entire Mackenzie Basin north of 60°N. A subsequent terrain sensitivity analysis identifies areas most susceptible to significant physical disturbance as a consequence of permafrost degradation. In addition, work has begun on more detailed high-resolution modeling (30m) in the vicinity of major communities within the Mackenzie Valley (e.g. Fort Simpson and Norman Wells). The high resolution work ultimately will be extended to the entire Mackenzie Valley Transportation Corridor, and is expected to require several more years for completion (depending on the pace of delivery of the final versions of the Landsat satellite-derived vegetation classifications).

Successful modeling of the spatial variability of ground temperatures (and thus the distribution of permafrost) depends upon i) the adoption of a numeric relation which

adequately describes linkages between the dominant climate and terrain factors influencing ground temperatures and ii) consolidation of a suitable database of geo-referenced information describing climate and terrain conditions at appropriate scales. This report presents an overview of the research conducted under CCAF project A073. Specifically it will:

- present the numeric model adopted in this work
- outline the development of spatial databases supporting ground thermal modeling at regional and local scales
- describe the derivation of appropriate values for model parameters
- summarize the results of modeling at both regional and local scales.

2 A NUMERIC MODEL OF THE GROUND THERMAL REGIME

Smith and Riseborough (1996) propose a simple numeric model as a powerful tool for investigating climate-permafrost relations. The model incorporates key environmental factors influencing ground temperatures, thus enabling prediction of the mean annual *temperature at the top of permafrost* (TTOP), under the assumption that thermal equilibrium has been achieved between the atmospheric and ground thermal regimes. Where permafrost does not exist, TTOP calculates the mean annual temperature at the base of the annual freeze-thaw layer. Ground thermal conditions are linked to the atmospheric temperature regime through the use of seasonal (summer and winter) n-factors (Lunardini, 1981), which offer a simplified representation of the influence of the buffer layer in modulating heat flow between the atmosphere and the ground surface.

$$TTOP = \frac{\frac{Kt}{Kf}\left(Ip \bullet Nt \bullet DDT - Nf \bullet DDF\right)}{P}$$

where:

TTOP	=	equilibrium temperature at the top of permafrost
K_t	=	thermal conductivity of unfrozen ground
K_f	=	thermal conductivity of frozen ground
DDT	=	air thawing degree days
DDF	=	air freezing degree days
n_t	=	summer n-factor
n_f	=	winter n-factor
I_p	=	potential insolation index
P	=	period (365 days)

Figure 2 presents a modeling template which aligns the TTOP numeric relation with the major aspects of climate and terrain deemed to be the dominant factors influencing the ground thermal regime (as proposed in the conceptual model of Figure 1).

Figure 2: A template for utilizing the TTOP relation for ground thermal modeling

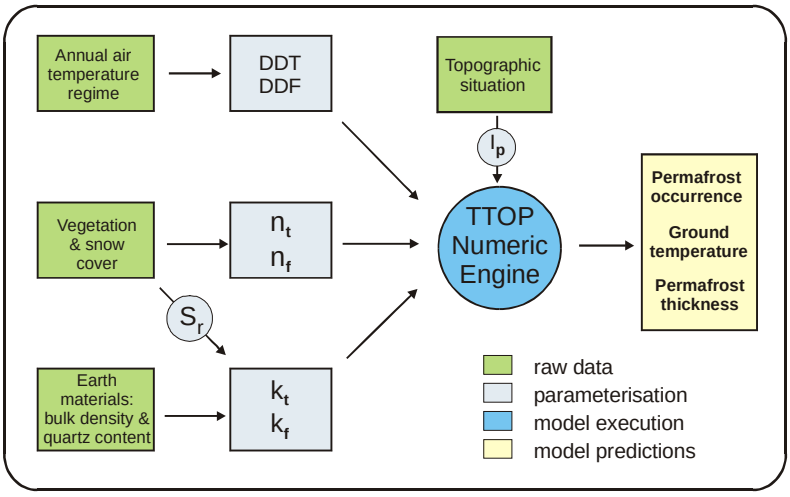

The successful application of this modeling approach depends primarily on two requirements:

1. The capacity of the numeric engine to generate accurate predictions of ground temperature within the constraints of *a priori* assumptions (technical performance).

2. the specification of model parameter values (on the basis of available information) which adequately represent climate and terrain conditions in the real world.

2.1 The Technical Performance of TTOP

The technical performance of the TTOP ground temperature model was evaluated through a comparison of TTOP predictions to those generated by a one-dimensional finite-element heat conduction model (T-ONE) developed at the National Research Council of Canada (Goodrich, 1978; 1982; personal communication, 1993). It is widely acknowledged that finite-element methods provide reliable solutions to complex problems by dividing space and time into discreet intervals (spatial grid, time steps), with an approximate numeric solution calculated at each time interval. In practice, the utility of finite-element methods for regional-scale investigations of permafrost has been limited by the excessive time required to calculate a solution for each unique condition of climate and terrain existing within very large study areas.

A range of arbitrary parameter values representing a variety of hypothetical site conditions (climate and terrain) were established as inputs to both the TTOP model and the T-ONE finite-element model. A uniform, single-layer substrate was assumed in order to maximize the compatibility of the TTOP and T-ONE models. For each set of parameter values, the T-ONE finite-element model was allowed to execute until thermal equilibrium between the atmospheric and ground thermal regimes was achieved (i.e. until

no further changes in ground temperature occur in successive time steps). In each case, the T-ONE prediction for the temperature at the top of permafrost was recorded, along with the corresponding TTOP prediction. Under these conditions, T-ONE results are directly comparable to the output of the TTOP model.

An analysis of outputs from both models indicates that the temperature at the top of permafrost corresponds closely to the minimum temperature achieved in the mean annual ground temperature profile (Figure 3) . At depths below the point at which this minimum occurs, the ground temperature profile is essentially linear (assuming a homogeneous substrate), and thus an estimate of the thickness of permafrost may be extrapolated directly from TTOP, based on the thermal conductivity of the substrate. This estimate can be adjusted for situations in which multiple layers having different thermal conductivity values are known to exist.

Figure 3: Generalized representation of a ground temperature profile through permafrost.

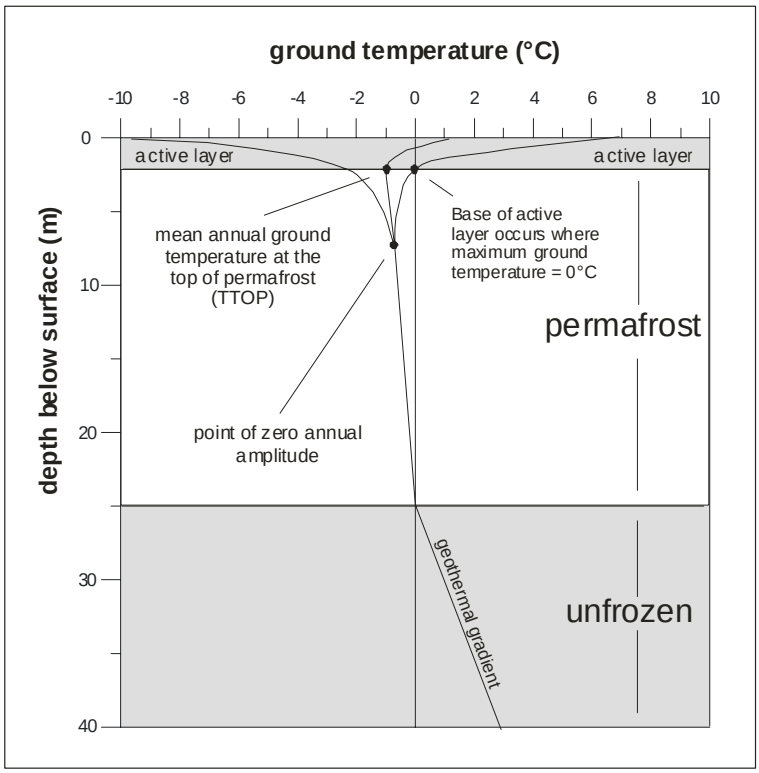

Figure 4 indicates that under the constraints specified, TTOP ground temperature predictions are in very close agreement with those obtained by finite-element methods. The comparison confirms that the TTOP relation provides accurate predictions of the equilibrium temperature at the top of permafrost for a wide range of hypothetical climate and terrain conditions.

Figure 4: A comparison of ground temperature predictions generated by the T-ONE finite element model and the TTOP relation

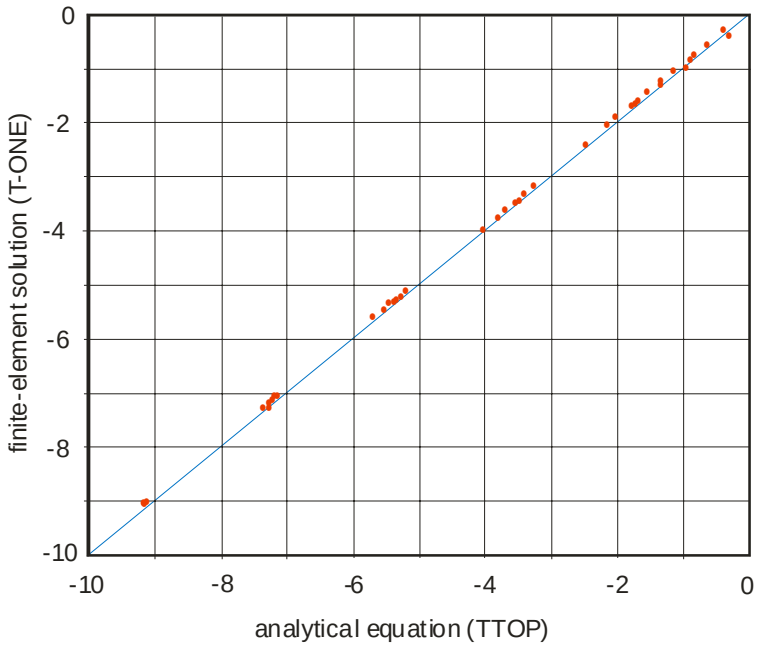

3 MODEL PARAMETERIZATION USING BOREHOLE DATA

It has been shown that TTOP performs well in a technical sense, within the limitations described in Section 2. However, in order to apply the model to regional-scale mapping of permafrost it is necessary to determine values for model parameters that adequately reflect climate and terrain conditions at representative sites within the study region. This requirement is critical for both site-scale and local/regional-scale modeling, and presents a significant challenge with respect to the application of TTOP (or any other physically-based ground thermal model) to permafrost mapping. Unfortunately, few data exist regarding the actual physical and thermal properties (e.g. soil density, thermal conductivity) of terrain in the Mackenzie River Valley. This is particularly true in the case of n-factors, for which only a very limited set of values has been proposed for vegetated surfaces. The alternative approach adopted in this work involved an iterative process of parameter adjustment, such that the number of correct TTOP predictions of the presence/absence permafrost was optimized within a dataset of 180 borehole observations of the ground thermal state along the Norman Wells Pipeline right-of-way (Figure 5). Borehole locations within the combined dataset span approximately 6° of latitude (over 600 km in north-south extent between Norman Wells and Zama, Alta.) and include a wide variety of terrain conditions considered to be generally representative of the broader Mackenzie River valley.

Figure 5: Site map showing the approximate location of the Norman Wells Pipeline right of way.

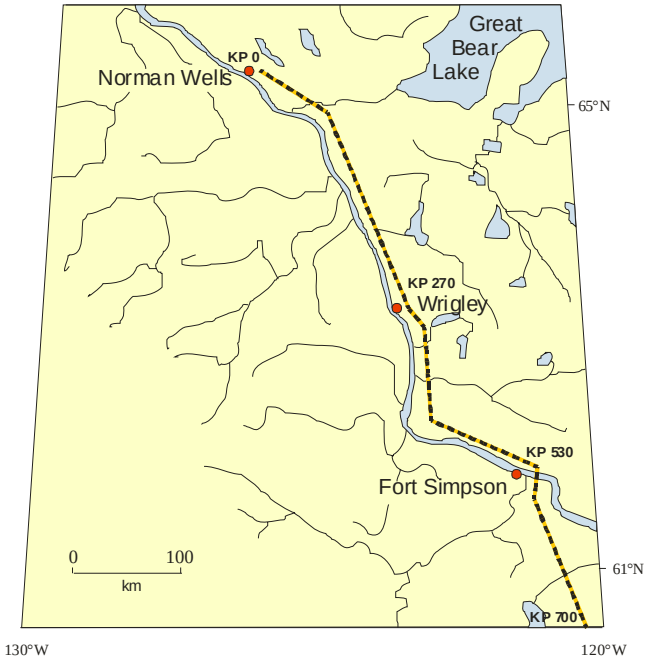

3.1 Borehole Records as a Source of Permafrost Data

Any assessment of the performance of a regional-scale ground thermal model is complicated by the fact that we know very little about the actual distribution of permafrost (other than a very generalized understanding at the national scale). Given that discrete observations of the presence or absence of permafrost are very sparse and generally limited spatially to particular areas of interest (such as oil exploration zones and transportation rights-of-way), we are unlikely ever to accumulate a sufficient number of site observations within any geographic region to generate statistical certainty regarding the distribution of permafrost. However, we can "calibrate" the model for application in a particular geographic region through iterative adjustment of individual model parameters such that the number of correct model predictions are optimised within a sufficiently large set of site observations of the presence/absence of permafrost (provided that adequate site descriptions are available).

3.1.1 Geotechnical borehole sites (un-instrumented)

A set of 154 geotechnical boreholes were selected from 270 boreholes drilled as part of a program to acquire stratigraphic data along the Norman Wells Pipeline alignment in support of engineering design applications (IPL, 1982a). Borehole records provided information about the dominant soil class at each site modeled, while additional information from IPL's geophysical survey (1982b) indicated the presence or absence of permafrost, and provided a generalized description of vegetation cover at each borehole

location. Selected boreholes were situated between KP 270 (just north of Wrigley, NWT) and KP 700 (south of Fort Simpson, NWT). Note that KP refers to the distance in kilometres, southward from Norman Wells along the pipeline right-of-way., To ensuring that all sites modeled were well within the discontinuous permafrost zone and that a balance was maintained between the number of permafrost/non-permafrost cases, geotechnical boreholes located north of KP 270 were excluded from the modeling. Records indicate that permafrost was present at 85 of 154 sites modeled (55%), with the remaining 69 sites being free of permafrost. Additional boreholes were excluded from the analysis if they were located in disturbed terrain, or if adequate descriptions of surficial materials and/or vegetation cover were lacking. Typically, maximum borehole depths were in the order of 10 metres (less if a refusal was encountered). Given that borehole records do not indicate the depth of freezing beyond borehole limits, only limited information about permafrost thickness could be inferred from this dataset.

3.1.2 Instrumented borehole sites

Records for an additional 26 boreholes were selected from a series of more than 100 boreholes drilled as part of a program established jointly by IPL and the Geological Survey of Canada to monitor ground thermal conditions along the pipeline right-of-way. These "thermal fences" consisted of 4 boreholes at each monitoring location, transecting the right-of-way at right angles to provide ground thermal data at various distances from the pipe. The boreholes were instrumented with 20 m temperature cables (Pilon et al., 1989), enabling researchers to estimate the thickness of permafrost at these sites based on interpolation/extrapolation of the ground temperature profile (Pilon et al., 1989), providing a basis for evaluating TTOP predictions of permafrost thickness. Selected boreholes were limited to those located some distance off the right-of-way adjacent to the pipeline, and were assumed to represent "undisturbed" site conditions. Permafrost was deemed to be present at 20 of 26 borehole sites (77%), with the interpreted thickness of permafrost ranging from about 3 m to 74 m.

3.2 Terrain Characterization and Data Generalization

Terrain characterization primarily involved the classification of surficial deposits and vegetation cover at each borehole location. The following sections briefly describe the derivation of a generalized classification scheme for each theme, and the determination of suitable model parameter values based on simplified descriptions of site conditions. Satisfactory optimisation of TTOP performance within the borehole dataset (in terms of the number of correct model predictions of the presence/absence of permafrost) will establish a basis for TTOP application to regional-scale mapping of the ground thermal state. The spatial modeling will employ the same classification schemes and associated parameter sets, but will utilise satellite imagery and available regional-scaled maps as primary data sources.

3.2.1 Surficial geology

IPL's (1982a) borehole logs included detailed descriptions of surficial deposits at borehole sites both in terms of distinctions between classes, and layering of units. It is

unlikely that such detailed information would be available from regional-scale maps, partly because of the prohibitive cost associated sampling large areas by drilling and coring, and the practical requirement to limit the number of classes for map display. Furthermore, during the compilation of paper maps spatial detail is often sacrificed in order to maintain reasonably contiguous thematic zones. Consequently, for regional-scale ground thermal modeling applications, the values assigned to model parameters will almost certainly be based on highly-generalized spatial data. For this work, descriptions of surficial geology at individual borehole sites have been limited to just seven primary classes (i.e. alluvial, colluvial, aeolian, glaciolacustrine, glaciofluvial, and glacial tills), with each class further subdivided according to soil texture (fine or coarse).

3.2.2 Vegetation cover

Information about vegetation cover at each of the 154 geotechnical borehole sites was extracted from a graphical interpretation of IPL's Continuous Geophysical Survey (1982b), which includes a summary of borehole characteristics along the ROW. For the set of 26 instrumented boreholes, a brief description of vegetation cover was included in the borehole documentation (Pilon et al., 1989). Vegetation classifications for both datasets were generalized to reflect the dominant vegetation unit, without reference to sub-units. Under this scheme, for example, both black spruce forest with minor white spruce, and black spruce forest with some poplar were classified as "black spruce". This scheme is generally consistent with classification schemes generated by multi-spectral analysis of satellite imagery and those accompanying existing area-class maps.

3.2.3 Organic terrain and peat cover

Typically, regional-scaled maps provide only crude estimates of the thickness of peat cover associated with organic terrain (bogs and fens), and usually only as broad ranges. Furthermore, terrain not specifically identified as organic nevertheless may be associated with significant deposits of peat in some cases (e.g.: an organic cover of moderate thickness is typically associated with black spruce forest stands). In the borehole modeling, the influence of relatively thin peat cover (less than 1 m in thickness) was assumed to be implicit in seasonal n-factors for selected terrain units. In cases where terrain was classed as non-organic but for which peat thickness in excess of 1m was indicated, thawing n-factors were reduced arbitrarily by a small amount (0.05) to account for the extra insulating effect of dry peat in summer (note that detailed information about peat thickness was available for the set of 26 instrumented boreholes only). Only terrain units identified specifically as bogs or fens were treated as truly organic terrain, for which the presence of a very thick peat cover was considered to be the dominant factor influencing the ground thermal regime.

3.2.4 Representation of regional climate

The influence of atmospheric climate on the ground thermal regime was assumed to be primarily a function of air temperature, as represented by thawing and freezing degree day indices. The modeling also assumes that heat transfer in permafrost terrain is dominated by conductive processes (Outcalt et al., 1990; Hinkle and Outcalt, 1994). Thus, heat transfer through convective transport of water vapour and air within soil pore

spaces (mass fluxes), and the transient influences of rainfall infiltration and surface runoff are not considered. The influence of snow cover was assumed to be implicit in the winter n-factor (following Jorgensen and Kreig, 1988). Note that in the absence of snow cover we would expect winter n-factors values to be very close to 1.0, given that vegetation cover in winter is generally very sparse.

A baseline climate for modeling (assumed to represent "current" climate conditions) was established by spatial interpolation/extrapolation of sparse point data collected at local community airports in Mackenzie River valley (1951-80 Climate Normals: Environment Canada, 1982). It was judged that this approach would reflect the comparatively stable climatic conditions prevailing for most of the 20th century, exclusive of the period of conspicuous warming in the latter decades.

3.3 Assignment of Model Parameter Values

Our modeling assumes that the generalized classification schemes describing surficial geology and vegetation cover are sufficiently detailed to enable the differentiation of ground thermal conditions for a limited set of representative terrain types. The following section describes the establishment of model parameter values representing the physical and thermal properties of terrain in the vicinity of each geotechnical borehole.

3.3.1 Estimating Thermal Conductivity

Few measurements of soil thermal conductivity specific to representative sites within the Mackenzie River Valley are currently available. In any case, spot measurements are of limited value for modeling purposes because soil thermal properties tend to be quite variable both spatially (vertically and laterally within a given soil unit) and temporally (across the seasons). The TTOP relation requires a single value representing the average seasonal thermal conductivity for each distinct terrain unit identified (i.e. each soil-vegetation combination). In order to impart a degree of rigour to the assignment of thermal conductivity parameters (K_t, K_f) for the various surficial geologic units, our modeling employs Johansen's (1975) equations for estimating frozen/unfrozen thermal conductivity based on the assumed physical and mineralogical properties of the soil substrate. Johansen's equations have been shown to generate reasonable results for a wide variety of natural mineral soils (Farouki, 1981). The generalised descriptions of surficial geology and vegetation cover serve as indicators of soil properties (i.e. bulk density, texture, mineralogy) and soil water content, respectively. Note therefore, that a range of thermal conductivity values are associated with each surficial soil unit, depending on the prevailing soil moisture conditions associated with the overlying vegetation.

Table 1 lists the physical properties assumed, and the seasonal thermal conductivity values assigned to the various surficial units. The bulk densities reported reflect average measured values obtained from recovered core samples along the pipeline right-of-way (IPL, 1982a). Quartz contents of 18% and 50% were assumed for fine-grained and coarser-grained soils respectively. Relative soil moisture contents at each site were inferred from the dominant vegetation cover type, following the premise that surface

vegetation is highly sensitive to the prevailing soil moisture regime. Jorgenson and Kreig (1988) provide guidelines for determining relations between vegetation cover and soil moisture conditions. In this work, soil water contents are described in terms of the degree of pore saturation (S_r), under the assumption that saturation levels imply an ordinal arrangement of water availability to plants (see Table 2 in the following section).

Table 1: Model parameters associated with various surficial soil units

Surficial Soil Unit	(Kg/m^3) Dry Density	(W/m/°C)	
		K_t	K_f
colluvial complex	1400	1.15-1.54	1.61-2.69
glaciolacustrine	1475	1.21-1.62	1.82-2.74
aeolian deposits	1500	1.39-1.60	1.63-2.47
glaciofluvial	1550	1.26-1.66	1.65-2.50
alluvial deposits	1600	1.30-1.72	1.59-2.53
glacial till	1750	1.41-1.98	1.68-2.92
organics (peatlands)	300	0.52	1.70

3.3.2 Deriving n-factor values

Surface vegetation and winter snow cover tend to modulate heat exchange between the atmosphere and the ground surface. The TTOP model accommodates this effect by modifying seasonal thawing and freezing air degree-day indices according to values of n_t and n_f. This provides a highly simplified expression of the combined influences of many heat transfer processes (e.g. conduction, convection, evaporation, transpiration) occurring continuously and/or seasonally within the buffer layer (Lunardini, 1981). An n-factor value of 1.0 suggests a barren or sparsely vegetated surface and therefore, no significant modulation of heat exchange at the ground surface. N-factor values approaching zero imply very strong modulation of heat flow.

Very limited n-factor data specific to vegetated surfaces are presented in Lunardini (1981) and Jorgenson and Kreig (1988), but neither source is specific to the Mackenzie valley. Taylor (1995) calculated n-factors for a number of sites in the Mackenzie River valley, based on a single year of temperature data. While these sources served as guides, n-factors calculated from short-term air/ground temperature data exhibit a high degree of variability both spatially (from site to site, region to region) and temporally (from year to year), and so are unlikely to adequately reflect the long-term influence of vegetation and snow cover on the ground thermal regime. The n-factors employed in this modeling (Table 2) were determined through iterative adjustment of initial values in successive model runs, such that an optimum number of correct model predictions were obtained within the set of 154 geotechnical boreholes. Assuming that Johansen's equations adequately "anchor" the model through the rigorous assignment of seasonal thermal conductivity values, we may consider that the derived n-factor values reflect the average long-term modulating effect of surface vegetation and snow cover (acting over decades to centuries).

Table 2: Model parameters associated with vegetation cover

Vegetation Cover	Jorgenson & Kreig		This Study		S_r
	n_t	n_f	n_t	n_f	
upland spruce	.80	.35	.80	.31	0.80
open black spruce	.60	.30	.60	.24	0.85
closed black spruce	.50	.30	.55	.24	0.80
pine	-	-	.80	.35	0.50
poplar (aspen)	1.00	.30	.90	.30	0.60
birch	.90	.35	.80	.35	0.70
alder (shrub)	.85	.30	.85	.30	0.70
sedge fens	-	-	.70	.12	1.00
peat plateau (raised bog)	-	-	.50	.14	1.00
mixed forest*	-	-	.85	.31	0.70
barren land (tundra)*	-	-	.67	.83	0.95

* class not represented in borehole dataset

3.3.3 Degree-day indices

A very simple method for describing the annual air temperature regime along the pipeline right-of-way was adopted for the borehole modeling. Mean annual air temperatures for Norman Wells, Wrigley and Fort Simpson (at KP 0, KP 270 and KP 531 respectively) were converted to thawing and freezing degree-day indices based on a sinusoidal annual temperature wave with an amplitude of 23 C°. Linear equations were fitted to the summer and winter data to describe the relations between seasonal degree-day indices and the KP location (Figure 6). Degree-day indices for individual borehole sites were obtained through interpolation or extrapolation of these relations. No attempt was made to adjust degree-day indices for differences in elevation or topographic situation within the set of 154 geotechnical boreholes. However, suitably-scaled data describing local relief were available for the set of 26 instrumented boreholes sites, allowing adjustment of summer degree-day indices to reflect the influence of terrain slope and aspect (following Lee, 1964).

Figure 6: Mean annual air temperatures in relation to the kilometer-post (KP) distance from Norman Wells

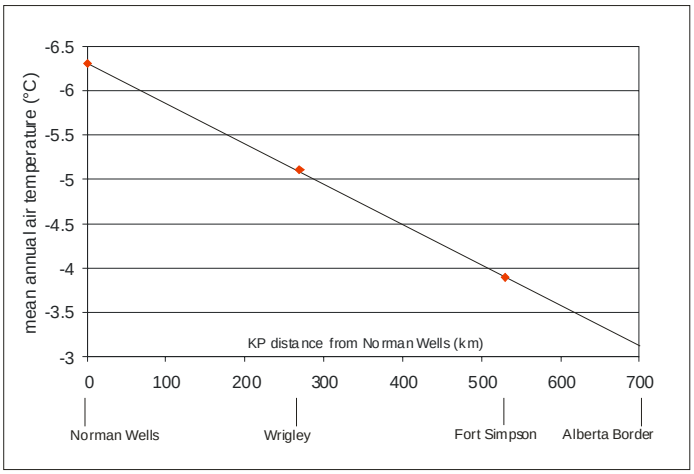

4 RESULTS OF TTOP MODELING AT BOREHOLE SITES

The TTOP model was initially applied to the set of 154 geotechnical boreholes using n-factor values which strongly reflected those employed in Wright's (1995) HPPM Model. The initial model run produced correct predictions of permafrost occurrence (the presence or absence of permafrost) at 75% of borehole sites. During subsequent runs, prediction accuracy within the dataset was optimized through iterative adjustment of individual parameter values (primarily n-factors). These "optimized" parameter values were subsequently applied to the set of 26 instrumented boreholes to evaluate TTOP predictions of the occurrence *and* thickness of permafrost at these sites.

4.1 TTOP Predictions of Permafrost Occurrence

In the previous section, a set of model parameter values was established which satisfactorily reproduced the observed distribution of permafrost within the borehole dataset, such that the presence or absence of permafrost was correctly predicted at 134 of 154 geotechnical borehole sites (87%). The "optimized" model performed well within the individual categories of vegetation cover and surficial geology (Tables 3 & 4) and with respect to additional partitioning of the dataset on the basis of latitude (location in the northern vs southern half of the pipeline right-of-way), and according to soil texture (Tables 5 & 6).

Table 3: Model results by vegetation category

Vegetation Category	# of sites	Observed PF distribution		# correct	% correct
		Frozen	Unfrozen		
black spruce	59	43	16	51	86.4
white (upland) spruce	40	23	17	36	90.0
pine	23	3	20	21	91.3
deciduous forest	20	8	12	15	75.0
bogs	7	6	1	6	85.7
fens	5	0	5	5	100.0
Overall	154	83	71	134	87.0

F = frozen U = unfrozen

Model results by vegetation category are presented in Table 3. Model predictions of the presence/absence of permafrost were better than 85% correct for all categories except deciduous forests, for which only 15 of 20 cases (75%) were correctly predicted. Sub-classes within this category consisted of poplar (13 sites), alder (2 sites) and birch (5 sites), with each assigned a unique set of n-factors and associated pore saturation levels. Clearly, the dataset contained too few cases within these sub-classes to impart a high level of confidence in the parameter values assigned. It is also possible that particularly deep seasonal frost may have promoted the misinterpretation of permafrost at some of the deciduous forest sites (note that permafrost was observed at 8 of 20 deciduous sites).

Table 4: Model results by surficial soil unit

Surficial Soil Unit	# of sites	Observed PF distribution		# of correct predictions	% correct
		Frozen	Unfrozen		
aeolian	12	4	8	10	83.3
alluvium	6	0	6	6	100.0
colluvium	20	16	4	20	100.0
glaciolacustrine	35	28	7	32	91.4
glaciofluvial	8	4	4	6	75.0
glacial till	61	25	36	49	80.3
organic	12	6	6	11	91.7
Overall	154	83	71	134	87.0

Table 4 presents TTOP modeling results by surficial geologic category. Correct predictions were obtained in 80-100% of cases within all categories, with the exception of glacialfluvial deposits (75% correct). It should be noted that there were only 8 cases in the glacialfluvial category (and only 6 boreholes were sited on alluvial deposits). Although 61 boreholes were sited on glacial till, it is likely that the relatively high degree of internal variability (with respect to physical/thermal properties of different till deposits) contributed to the comparatively modest prediction accuracy (80%) within this category.

The modeling results were further evaluated with respect to soil texture (Table 5) and borehole location within either the northern or southern portion of the pipeline right-of-way (Table 6), with correct predictions ranging from 85 to 89% within the specified categories.

Table 5: Model results by texture class

Texture	number of cases	number of correct predictions	% correct
Fine	88	75	85
Coarse	54	48	89

Table 6: Model results by kilometer post location

KP range	number of cases	number of correct predictions	% correct
270 – 450 (north)	76	65	86
450 – 700 (south)	78	69	88

Overall, the consistency apparent in the performance of the model within these several distinct data partitions makes it unlikely that the generally high level of prediction accuracy can be attributed to systematic bias within the borehole dataset (favoring either the presence or absence of permafrost in certain categories). We can therefore assume a reasonable measure of confidence that the parameterisation scheme employed in the modeling adequately reflects the influences of the major climate and terrain factors influencing the ground thermal state (i.e. the presence/absence of permafrost) within the geographical region represented by the borehole dataset. A summary of individual borehole site characteristics, assigned values for model parameters, and TTOP modeling

results for the set of 154 geotechnical boreholes is presented in spreadsheet form in Appendix 2.

4.2 TTOP Predictions of Permafrost Thickness

Modeling results for 154 Geotechnical borehole sites

Estimates of permafrost thickness are. TTOP predictions of the mean annual temperature at the top of permafrost were converted to corresponding estimates of permafrost thickness at each of the 154 geotechnical borehole sites (Figure 7) by extrapolating along the geothermal gradient to 0°C (refer to Figure 3). The slope of the geothermal gradient was established as a function of the frozen thermal conductivity of the substrate, and an assumed regional geothermal heat flux of 0.04 Wm^{-2}. A homogeneous substrate was assumed, such that no adjustments were made to account for possible layering of surficial materials with different physical/thermal properties (although adjustments could be made if suitable information were available). In general, model predictions of permafrost thickness in the Wrigley to Fort Simpson portion of the pipeline right-of-way are consistent with limited published data regarding permafrost thickness in the southern Mackenzie valley (Judge, 1973, 1975).

Figure 7: TTOP predictions of permafrost thickness for 154 geotechnical borehole sites along the Norman Wells pipeline right-of-way.

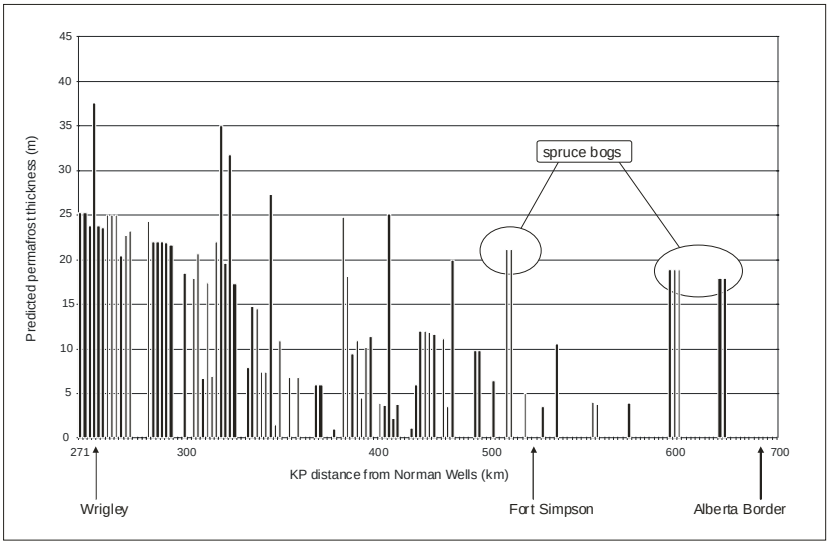

Modeling results for 26 instrumented borehole sites

Modeling results for the set of 26 instrumented boreholes are presented in Figure 8 and in spreadsheet format in Appendix 3. Parameter values assigned were consistent with those employed in the modeling of the larger set of 154 geotechnical boreholes. The model correctly predicted the presence/absence of permafrost in25 of 26 cases (96%). In

general, predictions of permafrost thickness agree favorably with estimates of permafrost thickness interpreted from ground temperature logs for these sites (Pilon et al., 1989), ranging from about 1 metre to just over 45 metres of permafrost.

The model appears to under-predict the thickness of permafrost at several sites located in the more northerly portion of the right-of-way in the vicinity of Wrigley, for which temperature logs indicate permafrost thickness of 50 metres or more. However, we note that 4 of these sites (84-3B, 85-7A, 85-7B, 85-7C) are located within a kilometre of each other, and may be influenced by unknown site factors or microclimatic conditions that are unaccounted for in the modeling.

We should consider the likelihood that at sites where thick permafrost is encountered, a general disequilibrium may exist the between the current atmospheric temperature regime and ground thermal conditions at greater depths. The occurrence of thick permafrost at these sites might therefore be a reflection of a period of cooler regional climatic conditions which prevailed a century or more ago (e.g. the Little Ice Age). If we assume a subsequent period of progressive warming to current conditions, we may speculate that thinner permafrost would have responded relatively quickly to increasing air temperatures and might thus be in a state of near-equilibrium with the prevailing climate. In contrast, we would expect that much longer time periods would be required to substantially degrade permafrost that extends to greater depths.

Figure 8: TTOP predictions of permafrost thickness at 26 instrumented boreholes located at pipeline monitoring stations along the right-of-way.

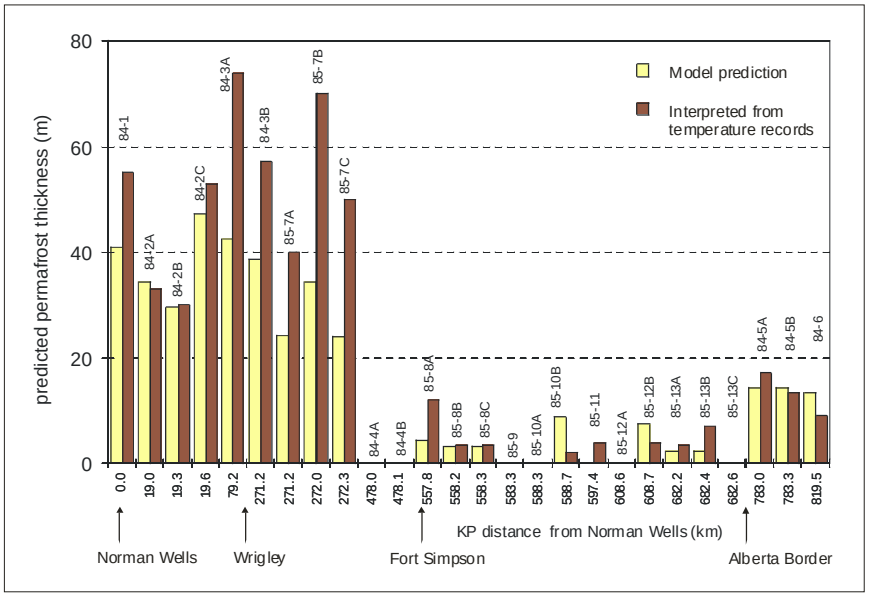

The modeling results suggest that it would be prudent to attach a relatively high degree of uncertainty to model predictions of relatively thin permafrost (those of less than 5 m or so), as in these cases we are dealing with predicted ground temperatures that typically are

within about a tenth of a degree the freezing point. A similar circumstance exists in cases where no permafrost is indicated because the TTOP model predicts ground temperatures marginally above 0°C. For example, the model failed to predict the presence of permafrost at borehole 85-11 (predicted ground temperature was 0.24°C), although 4 metres of permafrost was interpreted for that site. Also note that in cases where the presence/absence of permafrost is correctly predicted, relative errors can be high for predictions of thin permafrost, even though absolute errors are comparatively small (e.g. 85-18A & 85-10B). With respect to permafrost mapping applications, this uncertainty might be addressed through the inclusion of a "marginal" class indicating the possibility of thin permafrost. Furthermore, we should consider that the high degree of prediction accuracy within this dataset (96%) may be at least partly a consequence of the relatively small number of boreholes modeled, and the limited variety of site conditions represented.

5 MAPPING THE AREAL EXTENT OF PERMAFROST

Overall, the TTOP model correctly predicted the presence/absence of permafrost at 160 of 181 borehole sites (88.4%) within the combined borehole datasets. Values for model parameters were keyed to highly simplified classifications of surficial geology and vegetation cover, at a level of detail comparable to that generally inherent to currently-available regional-scaled maps. Such maps (together with ground cover classifications derived from satellite imagery) constitute core elements of the available spatial data that can practically be brought to bear on the problem of estimating the distribution of permafrost over extensive areas. The following sections describe the application of the TTOP model to regional-scaled mapping of the distribution and thickness of permafrost in the Mackenzie River Valley, Northwest Territories.

5.1 Spatial Data for Permafrost Modeling

A major objective of CCAF Project A073 is the consolidation of a digital spatial database of climate and terrain information in support of ground thermal modeling and route selection/evaluation applications in the Mackenzie River Valley. Access to suitable spatial data at appropriate scales is perhaps the most significant requirement for building a practical modeling capacity, even more so than the selection of a working model algorithm. Although a variety of options exist regarding the development of a working physical model, available options with respect to the acquisition of reliable spatial data are quite limited. This is particularly true for Canada's vast northern regions, as exemplified by the great distances between climate recording stations, and the reluctance (even in today's context of global climate change) to maintain the existing network intact.

Satellite-derived data

Satellite-based systems are increasingly being used to monitor the physical characteristics of the earth's surface. Conventional mapping of surface vegetation cover has never been conducted for extensive regions of the arctic, although a detailed air photo-derived vegetation classification was produced for a narrow corridor along the Mackenzie River

as part of preparedness planning for the defunct Mackenzie Valley gas pipeline proposed in the 1970's (Environmental Social Program, 1974). Employing this type of mapping over large regions would be very time consuming and prohibitively costly in today's context. Alternatively, satellite imagery offers the benefit of a generally good spatial discrimination with respect to the variability in surface conditions, within the resolution range of the particular sensor/platform array. This raster-based data format can be seen as a substantial improvement in spatial discrimination as compared to conventional area-class (polygon) maps produced at comparable scales, which tend to represent relatively large areas as a single uniform class. For example, the NOAH AVHRR sensor system can differentiate 1 km x 1 km pixels, which is suitable for modeling over very large areas (although the relatively coarse ground resolution tends to result in more averaging of surface reflectance values than is desirable), while for sub-regional or local-scale modeling, Landsat systems are able resolve 30 m pixels, generally allowing more precise thematic discrimination of ground surface conditions at these finer scales.

However, confidence in the thematic accuracy of vegetation classifications derived from satellite imagery is modest at best. This is partly because the surface reflectance values apparent from the vantage point of the satellite platform are sensitive to a variety of atmospheric conditions (such as haze, clouds and shadow) making it difficult to consistently apply the same classification algorithms to adjacent images, or even within the same image. Even under ideal atmospheric conditions, surface cover classifications produced by correlation of multi-spectral reflectance values to known vegetation types occurring at a series of ground truthing sites suffers from the fact that more than one distinct class of ground cover may exist within the boundaries of any given pixel of interest. This is especially true for the low resolution data, for which reflectance values are averaged across comparatively large pixels. This situation often results in misclassification, or alternatively, in the creation of a set of ambiguous classes representing mixtures of various ground cover types. The recent development of new sensors with greater spatial and spectral resolution offer the potential for improved performance of satellite-based imaging and classification systems in the future, although the cost of acquiring coverage over large geographic areas can still be prohibitive to many users.

Notwithstanding these difficulties, satellite-derived vegetation classifications constitute key elements of the GSC ground thermal modeling database. The basic classifications provided by the Canada Centre for Remote Sensing (1 km low-resolution data) and by our GNWT partners (30 m high-resolution imagery) have been further enhanced by GSC researchers through integration of ancillary information acquired from conventional area-class maps (where available), as described in subsequent sections of this report.

Conventional area-class maps

Most of the available spatial data for Canada's northern regions exist in the form of conventional area-class maps, produced at relatively small scales and which display little local detail. National-scale information about the distribution of surface vegetation is generally limited to a few such sources, such as the eco-region and eco-zone map series which describe vegetation assemblages occurring within polygonal boundaries rather than delineating the location of specific vegetation types. As such, these data are poorly

suited to modeling applications which strive to differentiate ground temperatures on the basis of distinct classes of vegetation cover. A notable exception is the Environmental Social Program Map Series ESP-101 entitled "Vegetation Types of the Mackenzie Valley Corridor" (1974), which provides detailed information about forest cover types (height, density, species) in a narrow north-south corridor spanning the Mackenzie River between the Beaufort Sea and the Alberta border. The dataset has contributed substantially to this project, with the ancillary information about species differentiation being incorporated into enhanced satellite-derived vegetation classifications (especially with regard to the discrimination of different coniferous forest types). Approximately 30 ESP map sheets (1:125,000) covering the entire so-called Mackenzie Valley Transportation Corridor were digitized, georeferenced, and integrated into the ground thermal modeling database.

5.2 Regional-scale Modeling with Low-resolution Data

The low-resolution database supporting geothermal modeling of the broader Mackenzie River Valley between 60°N (Alberta border) and 70°N (Beaufort Sea) consists of:

1. 1km x 1km land cover classification for Canada (Figure 9) produced by the Canada Centre for Remote Sensing based on multi-spectral AVHRR imagery acquired by the NOAH series of geostationary orbiting satellites (CCRS, 1999).

2. Digital version of 1:1,000,000 scale surficial geology maps of the Mackenzie Valley and adjacent areas (Figure 10), 60°N-64°N and 64°N-70°N (Aylsworth et al., GSC Bulletin 547, 2000).

3. Digital versions of 1:2,000,000 scale maps showing the distribution of organic terrain in the Mackenzie Valley (Aylsworth and Kettles, GSC Bulletin 547, 2000).

4. A digital elevation model (DEM) of the broader Mackenzie River valley compiled from NTDB (National Topographic Database) products and re-sampled to 1km resolution (Figure 11).

5. Spatial interpolation of thawing and freezing degree-day indices for the Mackenzie Valley based on 1951-1980 Climate Normals (Environment Canada, 1982).

On the basis of the borehole modeling results, spatial modeling proceeded under the assumption that the parameter values presented in Tables 1 & 2 adequately differentiate terrain conditions within the Mackenzie River valley with respect to the influences of surficial geology and surface vegetation cover on the ground thermal regime. Therefore, the spatial modeling dataset was reorganized (through reclassification/integration of individual data layers) to be compatible with the model parameters previously established. Additional influences of terrain slope and aspect were represented by a potential insolation index (Ip) following Lee (1964), which was applied as a multiplier to the summer degree day index. A digital elevation model (DEM) of the broader Mackenzie River valley (Figure 11) formed the basis for the calculation of Ip.

Regional vegetation data extracted from AVHRR Satellite Imagery classified by the Canada Centre for Remote Sensing (Cihlar and Beaubien, 1998) for the Northern BIOsphere and Modeling Experiment (NBIOME).

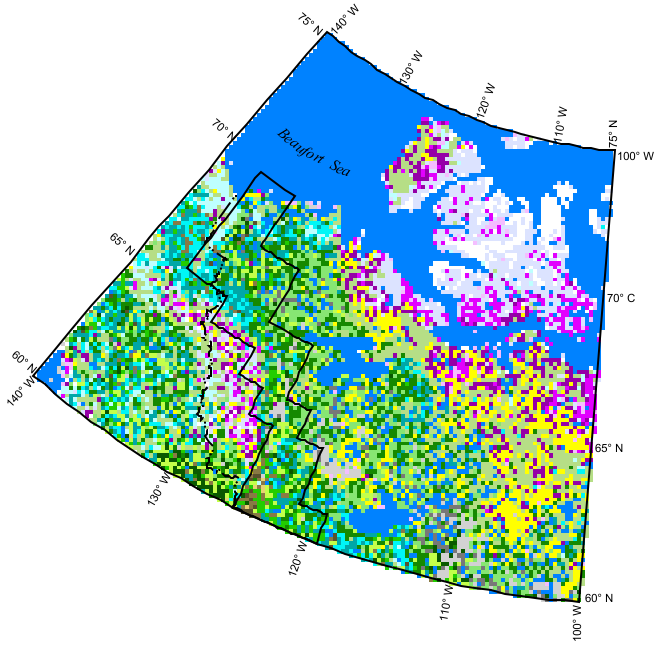

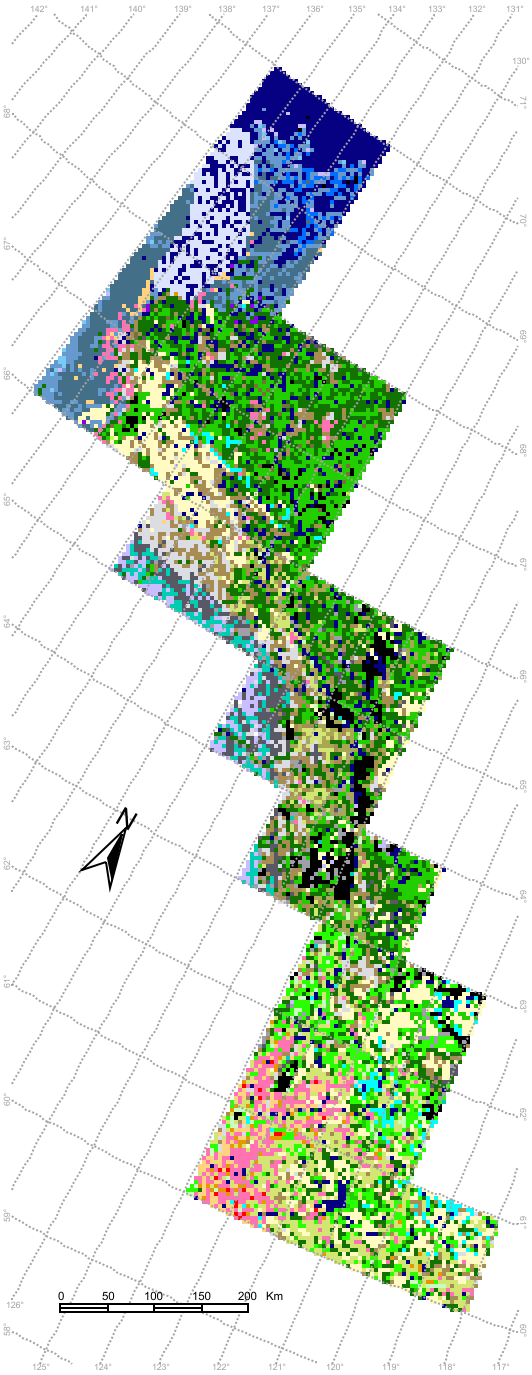

The CCRS satellite classification was enhanced using the Environmental Social Program Map Series 101 (ESP, 1974) and information about organic terrain (Aylsworth et al., 2000).

- Evergreen\High Density - Mixed Conifer
- Evergreen\Medium Density - Mixed Conifer
- Evergreen\Low Density - Mixed Conifer
- Evergreen\High Density - Black Spruce
- Evergreen\Medium Density - Black Spruce
- Evergreen\Low Density - Black Spruce
- Evergreen\High Density - White Spruce
- Evergreen\Medium Density - White Spruce
- Pine
- Mixed Closed Canopy Forest
- Mixed Needleleaf Forest - Spruce Dominated
- Mixed Broadleaf Forest
- Transition Treed Shrubland
- Transitional Forest -- Evergreen - Black Spruce
- Transitional Forest -- Evergreen - Mixed Conifer
- Mixed Patchy Distribution
- Fen - Extensive
- Bog - Extensive
- Upland Tall Shrubland
- Riparian Shrubland (wet areas)
- Wetland-Shrubland
- Low Vegetation Cover
- Bare Soil and Rock
- Burn Areas
- Tundra -- Burn Areas
- Tundra -- Wetland-Shrubland
- Tundra -- Upland Tall Shrubland
- Tundra -- Low Vegetation Cover
- Tundra -- Wet baren land
- Modern Delta
- Snow or Ice
- Waterbodies

Surficial geology of the Mackenzie River Valley (Aylsworth, 2000). Map information was used to define material parameter values (bulk density, texture and mineralogy).

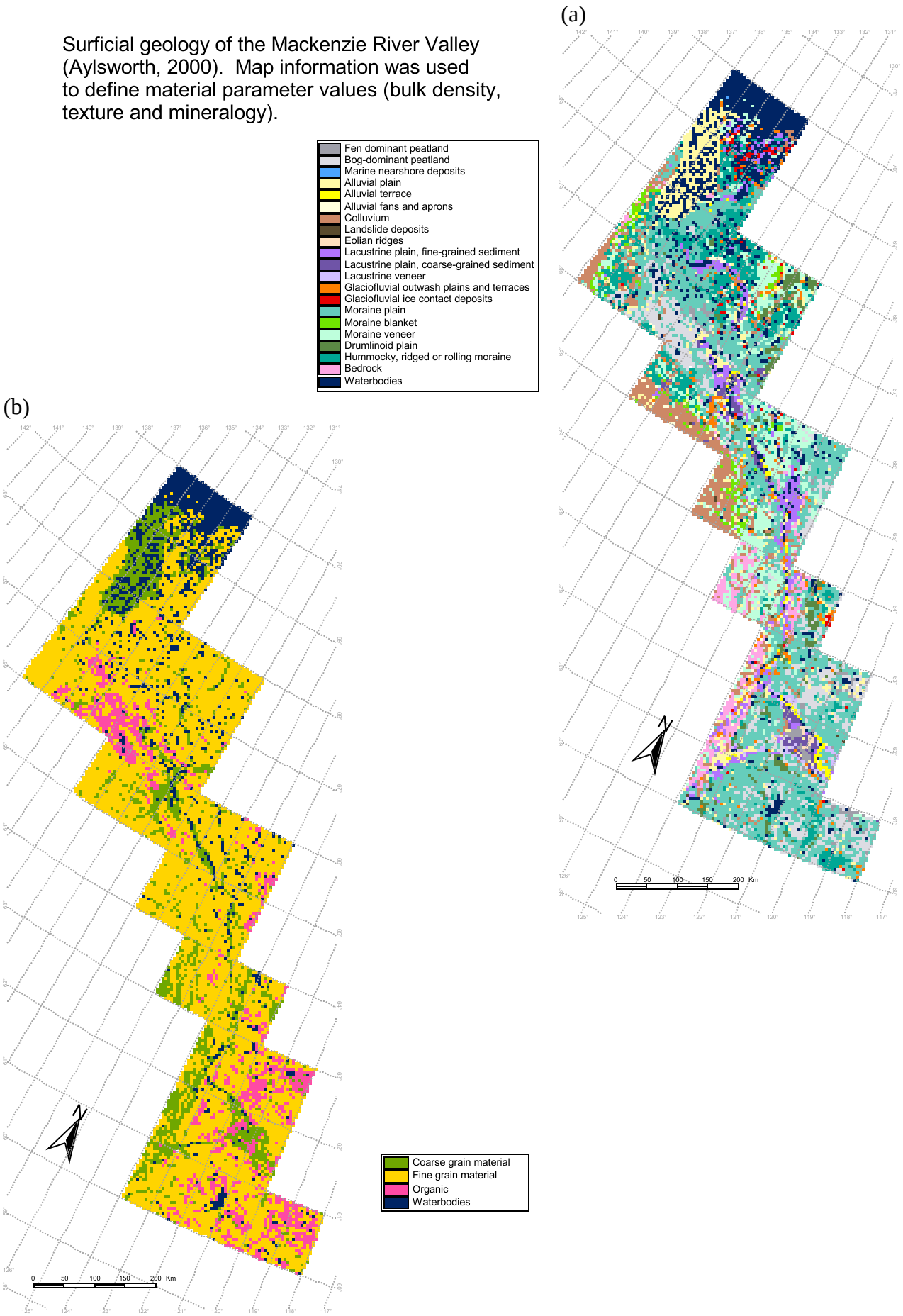

Figure 11

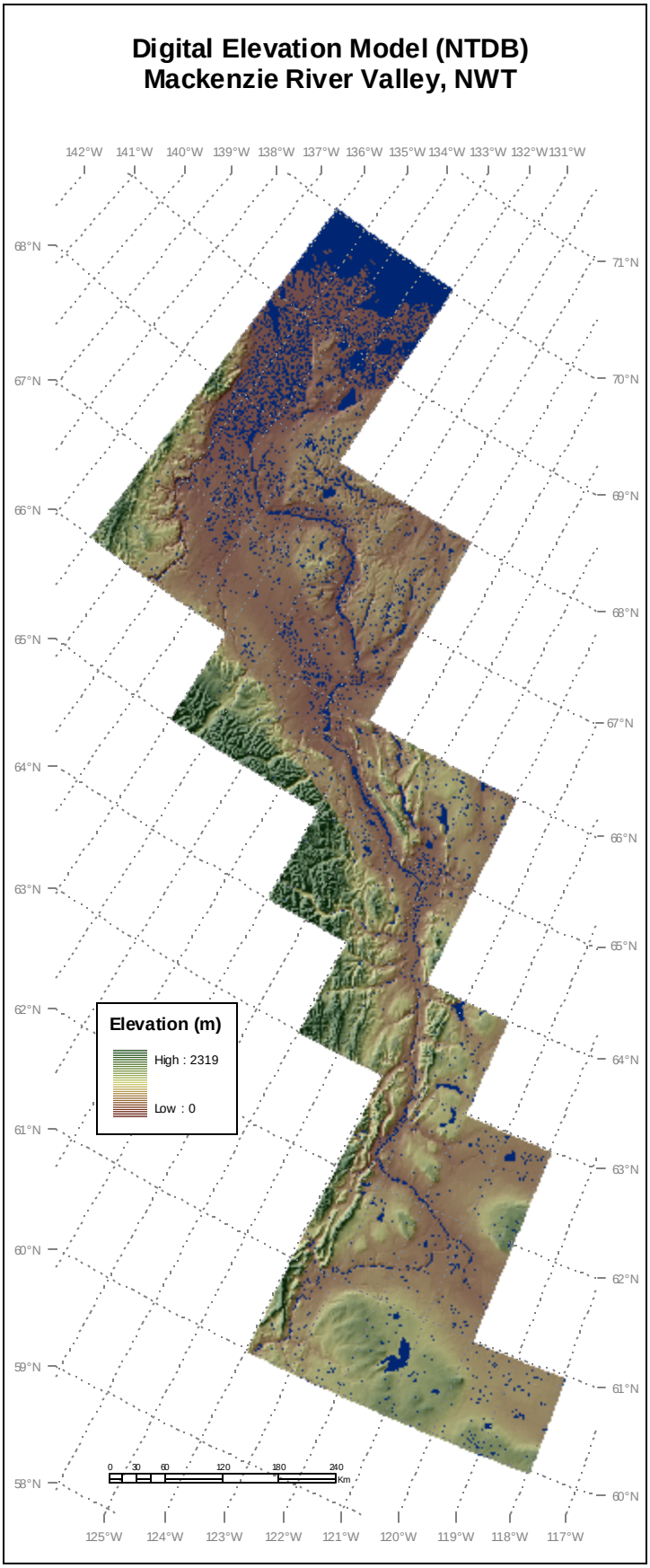
Digital Elevation Model (NTDB)
Mackenzie River Valley, NWT
142°W 141°W 140°W 139°W 138°W 137°W 136°W 135°W 134°W 133°W 132°W 131°W
68°N
67°N
66°N
65°N
64°N
63°N
62°N
61°N
60°N
59°N
58°N
71°N
70°N
69°N
68°N
67°N
66°N
65°N
64°N
63°N
62°N
61°N
60°N
125°W 124°W 123°W 122°W 121°W 120°W 119°W 118°W 117°W
Elevation (m)
High : 2319
Low : 0
0 30 60 120 180 240
Km

Figure 12

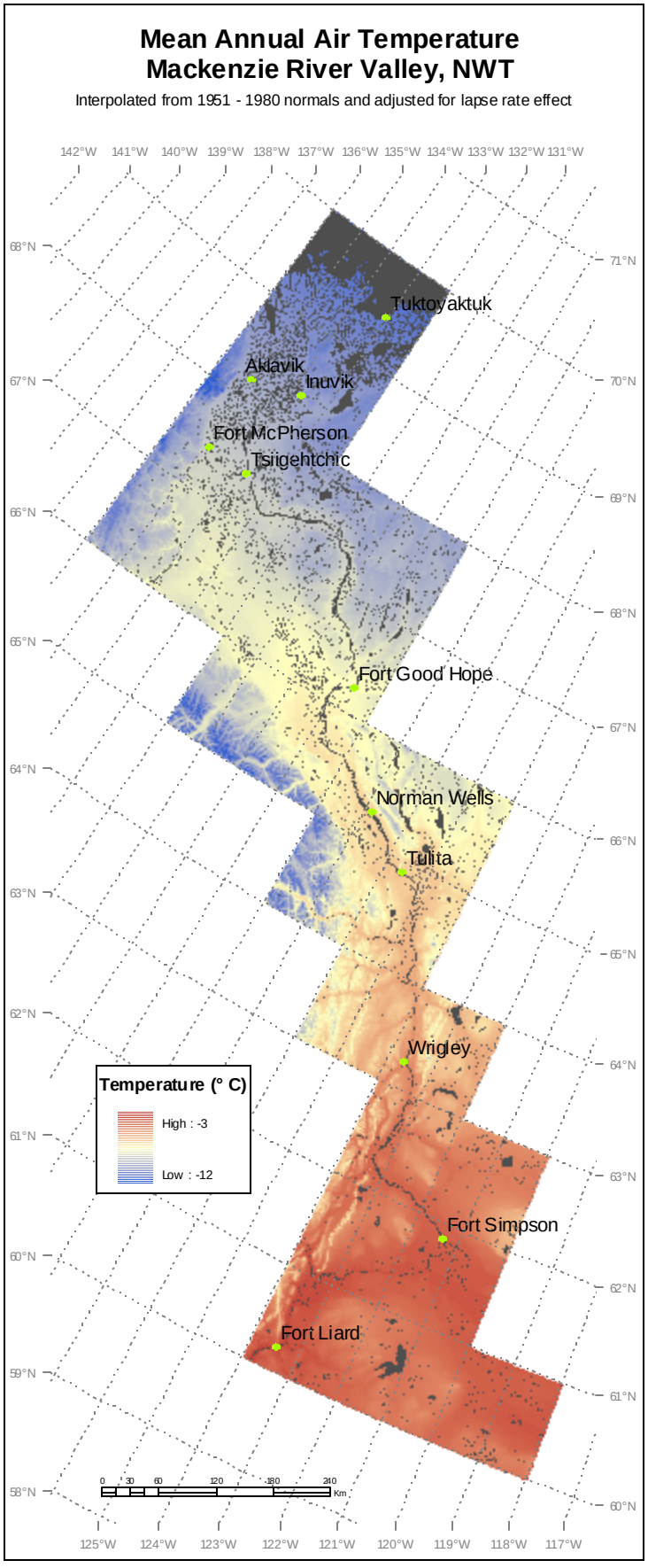
Mean Annual Air Temperature
Mackenzie River Valley, NWT
Interpolated from 1951 - 1980 normals and adjusted for lapse rate effect
142°W 141°W 140°W 139°W 138°W 137°W 136°W 135°W 134°W 133°W 132°W 131°W
68°N 67°N 66°N 65°N 64°N 63°N 62°N 61°N 60°N 59°N 58°N
71°N 70°N 69°N 68°N 67°N 66°N 65°N 64°N 63°N 62°N 61°N 60°N
125°W 124°W 123°W 122°W 121°W 120°W 119°W 118°W 117°W
Tuktoyaktuk
Aklavik
Inuvik
Fort McPherson
Tsiigehtchic
Fort Good Hope
Norman Wells
Tulita
Wrigley
Fort Simpson
Fort Liard
Temperature (° C)
High : -3
Low : -12
0 30 60 120 180 240
Km

5.2.1 Assigning parameter values to spatial data

Vegetation cover

The vegetation classification employed in the low resolution modeling is presented in Figure 9. These data are based strongly on a surface cover classification produced by the Canada Centre for Remote Sensing (CCRS, 1999), however the classification has been enhanced through cross-tabulations with tree species information from the Environmental Social Program (ESP) Map Series 101 (1974). Values for seasonal n-factors (nt, nf) and soil moisture content (S_r) were obtained by relating individual map classes to the vegetation categories presented in Table 2. In the case of mixed conifer-deciduous forests n-factor values intermediate to those of "pure" forest species were assumed (note however, that at 1 km resolution this class may often consist of a patchwork of relatively pure decidous/conifereous stands) In cases where forest cover is mixed but considered to be dominated by a particular species, n-factor values associated with the dominant species were employed.

Surficial geology

Figure 10a presents the classification of surficial geology (Aylsworth et al., GSC Bulletin 547, 2000) used in the low resolution modeling of the entire Mackenzie River valley, north of 60°N latitude. Figure 10b indicates the texture of mineral soils (coarse or fine grained) and the distribution of organic terrain. The classification is compatible with the surficial geologic categories presented in Table 1, and thus enables the assignment of model parameter values representing soil bulk density, soil mineralogy, and soil texture, which were subsequently employed in Johansen's (1975) empirical equations for estimating the frozen and unfrozen thermal conductivity of mineral and organic soils.

Digital elevation models

A digital elevation model of the entire study area was compiled from NTDB data (national coverage available as individual NTS map sheets, nominally at 500m grid resolution) and subsequently re-sampled to a pixel resolution of 1 km (Figure 11). Elevation data are required for the calculation of a potential insolation index (Ip), which adjusts summer degree day indices to reflect the modulating effect of terrain slope and aspect on the amount of solar insolation received at each grid location. Digital elevation data also facilitated the incorporation of lapse rate effects in the modeling.

Regional climate

Reliable information about regional climate is lacking for most of the Mackenzie River valley. Daily weather information is collected systematically by Environment Canada at only a few sites, mainly at airports in the vicinity of major communities along the river. Environment Canada's 1951-1980 Climate Normals (1982) served as the baseline climatic representing "current" conditions in the Mackenzie River valley. Daily air temperature information, expressed as freezing and thawing degree-day indices (DDF and DDT, respectively) serve as inputs into the TTOP model. Given that the model

assumes that ground temperatures are in thermal equilibrium with the atmospheric temperature regime, we must therefore assume that the current distribution of permafrost in the Mackenzie River valley is a reflection of a stable climate as expressed by the 1951-1980 Climate Normals. Values of DDF and DDT for each weather station were plotted against station latitude, and subsequently fitted with a 3rd degree polynomial to obtain a numeric relation describing the seasonal variation in air temperatures (as expressed in degree-days) within the north-south extent of the study area. Degree-day indices were subsequently adjusted for elevation effects, with a cooling of 0.3°C per 100 m of elevation assumed (50% of the normal lapse rate). Combining the interpolated station data and lapse rate adjustments produced maps of freezing and thawing degree day indices for the Mackenzie valley. For presentation purposes, the degree day maps have been recombined into a single map depicting mean annual air temperature adjusted for elevation effects (Figure 12).

5.2.2 Results of low-resolution regional-scale modeling

TTOP estimates of ground temperature

Figure 13 presents initial TTOP model estimates of ground temperatures in the Mackenzie River valley, under the baseline climate scenario represented by the 1951-1980 Climate Normals (Environment Canada, 1982). Specifically, these estimates refer to the temperature at the top of permafrost (TTOP) in cases where permafrost is present, or alternatively, to the temperature at the base of the seasonal frost layer if no permafrost exists. Recall that under conditions of thermal equilibrium, this closely corresponds to the minimum temperature achieved in the mean annual ground temperature profile (Figure 3). The modern (active) Mackenzie delta has been excluded from the modeling (due to the presumed dominance of non-conductive heat fluxes), as was all terrain above 700 m elevation. TTOP predictions of ground temperature ranged from about -0.5 to +2°C at the Alberta/NWT border, to colder than –10°C at the northern edge of Richards Island and the Tuktoyaktuk Peninsula. In general terms, the north-south distribution of ground temperatures as estimated by TTOP agrees very favorably with limited ground temperature data for the Mackenzie valley presented by Judge (1973), and with a larger number of ground temperature measurements in the GSC's Ground Temperature Database for Northern Canada (Smith and Burgess, 2000). Note that these relatively few ground temperature measurements are not ideally suited for comparison to model estimates due to i) the limited range of terrain types they represent locally, ii) uncertainties with respect to the depths at which temperatures were measured relative to the location of the top of permafrost, and iii) the lack of accurate site descriptions to accompany the temperature data. Considering that local/regional terrain conditions tend to be highly variable over relatively short distances, we cannot expect spot measurements of ground temperature to adequately convey the range of ground temperatures occurring in any local area or region. On the other hand, the high level of generalization of the spatial datasets used for derivation of model inputs limits the ability of the low resolution modeling to capture the full range of variability locally.

Temperature at the Top of Permafrost
Mackenzie River Valley, NWT

Baseline climate scenario

(Preliminary)

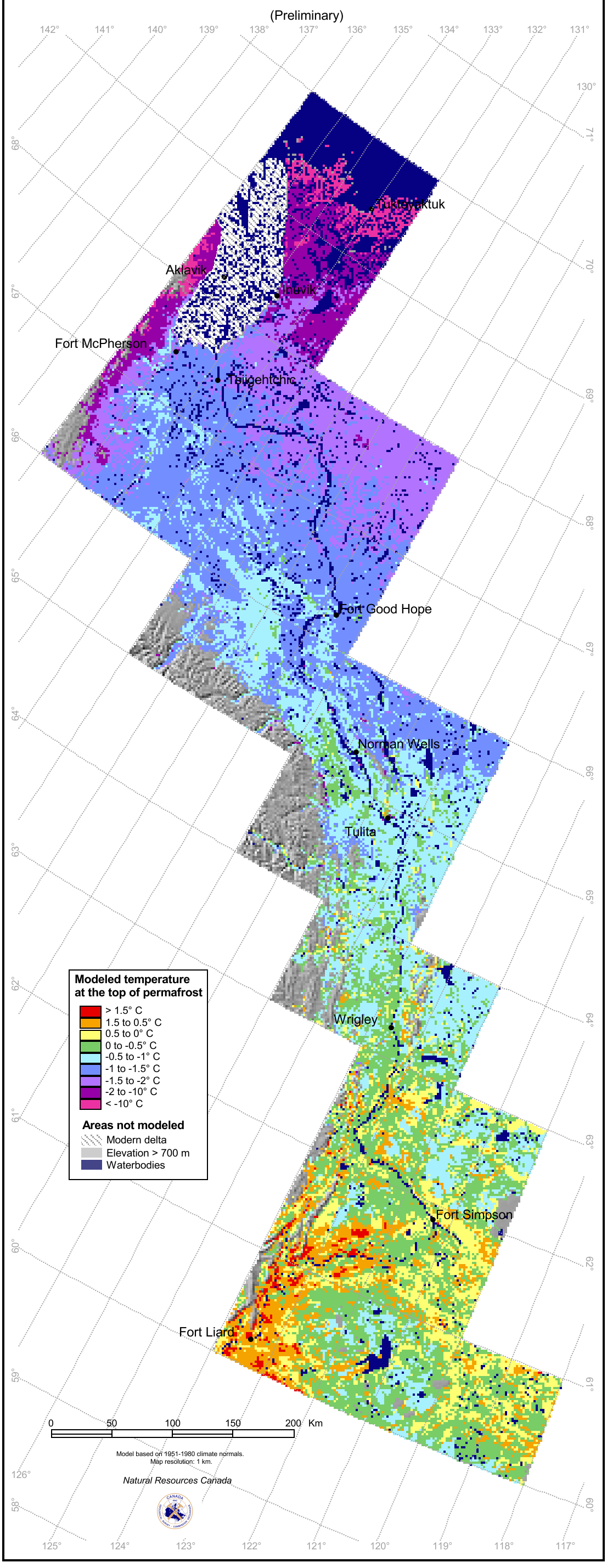

Figure 13

Predictions of permafrost thickness

TTOP ground temperature estimates were converted to predictions of permafrost thickness (Figure 14) by extrapolating along the assumed geothermal gradient to the depth at which it crosses the 0°C threshold. Geothermal gradients were calculated according to the thermal conductivity of the substrate, and an assumed value of the geothermal (terrestrial) heat flux. The accepted global average value of 0.05 Wm^{-2} was assumed for the coastal tundra regions of Richards Island and the Tuktoyaktuk Peninsula, while a lesser value of 0.04 Wm^{-2} was applied to the Mackenzie Valley proper, based on regional ground thermal data presented in Judge (1973). Estimates of permafrost thickness derived from TTOP ground temperature predictions agree favorably with limited data available for the Mackenzie Valley (Judge, 1973). Visual interpretation of Figure 14 suggests that permafrost becomes essentially continuous somewhere between Norman Wells and Fort Good Hope. This observation is in good agreement with the placement of the boundary between extensive discontinuous and continuous permafrost on Hegginbottom's (1995) permafrost map for Canada. Note that the maps produced to date should be considered as preliminary products, subject to revision following acquisition of the final versions of the Landsat vegetation classifications from the GNWT. Additional ground truthing of model predictions will also be undertaken over the next 2-3 years in an attempt to verify model performance with respect to regional-scale permafrost mapping applications.

Permafrost response to alternative climate scenarios

Figure 15 presents model predictions of the equilibrium distribution and thickness of permafrost under two scenarios of climate warming (i.e. 2°C & 4°C step increases in MAAT). The modeling suggests a dramatic change in the distribution of permafrost under a 4°C air temperature warming, assuming that the warmer climate persists for sufficient time to allow ground temperatures to equilibrate with the warmer atmospheric conditions. Ancillary finite-element modeling indicates that the relatively thin (less than 10 m) permafrost occurring in the southern portions of the Mackenzie valley can be expected to respond relatively quickly to a warming climate (perhaps within several decades to a century). However, for occurrences of very thick, cold permafrost (such as that which occurs in the Beaufort coastal regions) many thousands of years may be required to re-establish thermal equilibrium between the atmospheric and ground thermal regimes. A new 3-year PERD project has been approved to investigate the transient responses of permafrost terrain to regional climate warming.

Terrain sensitivity to climate warming

Figure 16 presents a map depicting terrain sensitivity to climate warming. A simple sensitivity index was adopted which accounts for predicted changes in ground temperature and permafrost thickness, and the potential physical response of the various surficial materials (mineral and organic soils) as ground temperatures gradually increase. The results are very preliminary and are presented here only as an example of the type of secondary product that can be generated from regional-scaled physically-based modeling of the ground thermal regime. A new 3-year GSC project has been approved to

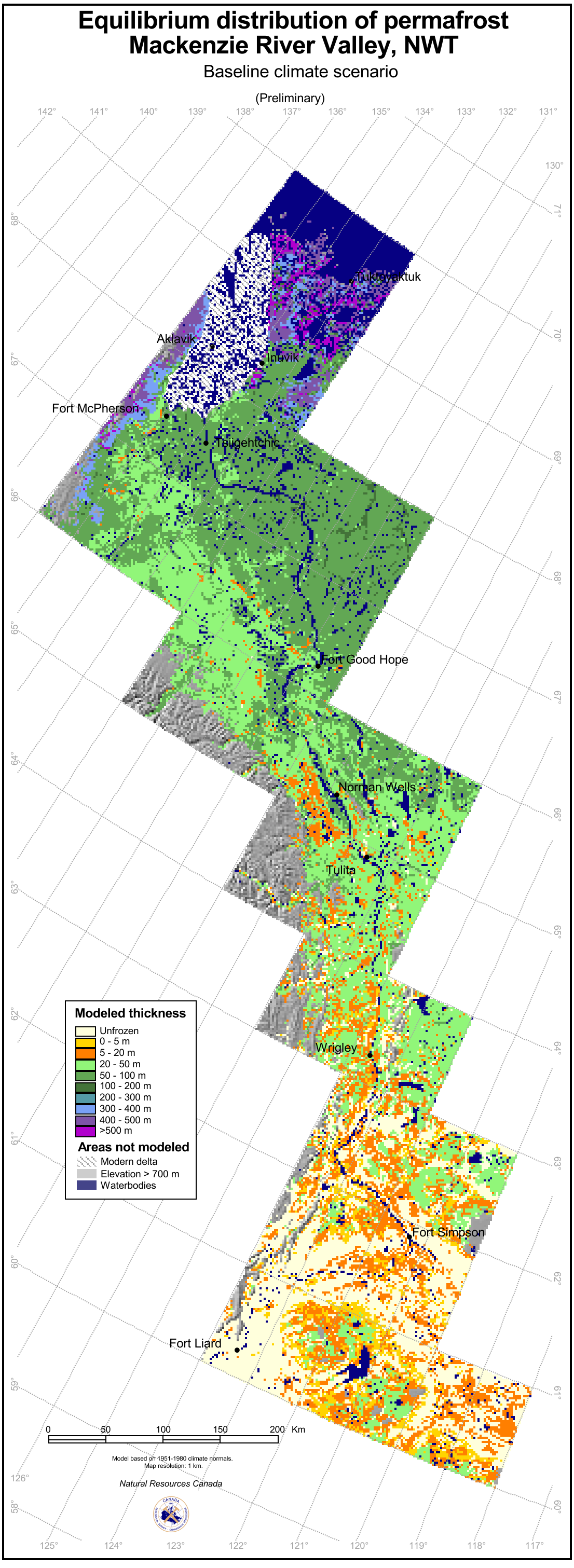
Equilibrium distribution of permafrost
Mackenzie River Valley, NWT
Baseline climate scenario
(Preliminary)
Tuktoyaktuk
Aklavik
Inuvik
Fort McPherson
Tsiigehtchic
Fort Good Hope
Norman Wells
Tulita
Wrigley
Fort Simpson
Fort Liard
Modeled thickness
Unfrozen
0 - 5 m
5 - 20 m
20 - 50 m
50 - 100 m
100 - 200 m
200 - 300 m
300 - 400 m
400 - 500 m
>500 m
Areas not modeled
Modern delta
Elevation > 700 m
Waterbodies
0 50 100 150 200 Km
Model based on 1951-1980 climate normals.
Map resolution: 1 km.
Natural Resources Canada

Figure 14

Equilibrium distribution of permafrost under three climate scenarios, Mackenzie River Valley, NWT

(Preliminary)

Figure 15

Baseline climate (derived from 1951-1980 normals)

2° C warming scenario

4° C warming scenario

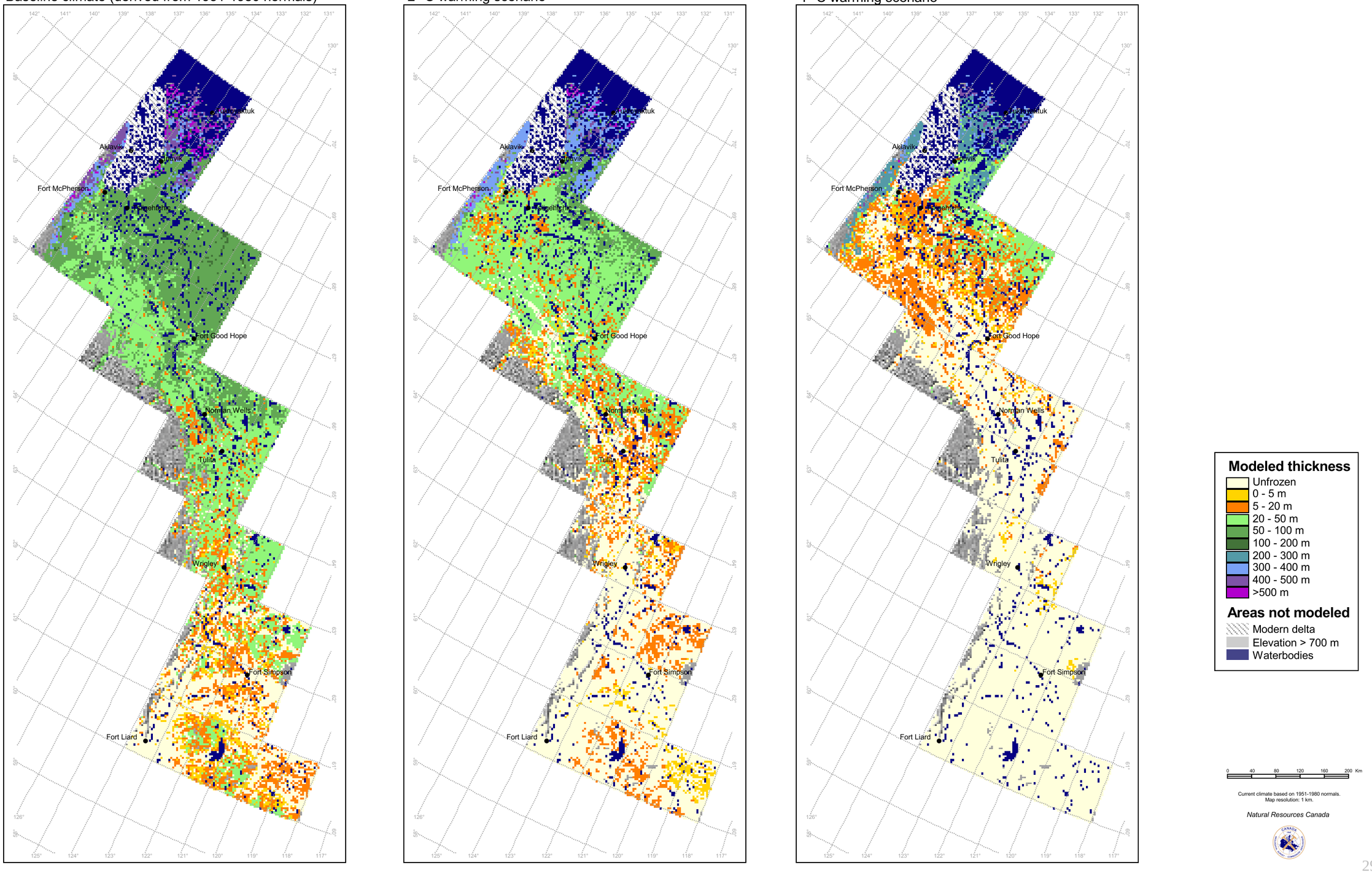

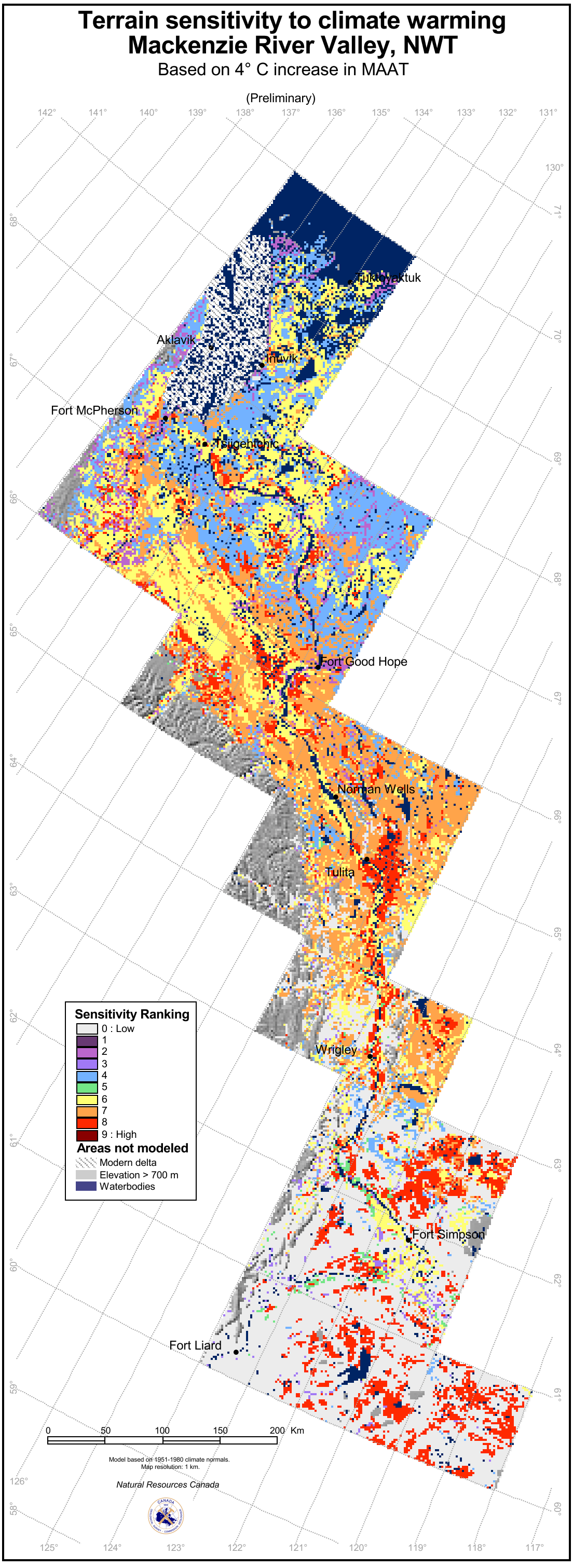
Terrain sensitivity to climate warming
Mackenzie River Valley, NWT
Based on 4° C increase in MAAT
(Preliminary)
Aklavik
Inuvik
Fort McPherson
Tsiigehtchic
Fort Good Hope
Norman Wells
Tulita
Wrigley
Fort Simpson
Fort Liard
Sensitivity Ranking
0 : Low
1
2
3
4
5
6
7
8
9 : High
Areas not modeled
Modern delta
Elevation > 700 m
Waterbodies
0 50 100 150 200 Km
Model based on 1951-1980 climate normals.
Map resolution: 1 km.
Natural Resources Canada

Figure 16

specifically address the issue of terrain sensitivity to climate warming in the Mackenzie River valley.

5.3 Spatial Modeling using High-Resolution Data

The low-resolution spatial modeling (1 km pixel resolution) described in previous sections produced a reasonable estimation of ground thermal conditions in the Mackenzie River valley, and thus enables prediction of the distribution and thickness of permafrost, from a broad regional perspective. As a physical model, TTOP defines explicit linkages between the atmospheric climate regime and the ground thermal state, and therefore is well suited to the investigation of the impacts of climatic change on permafrost. On a regional basis, the low-resolution modeling can serve as a useful tool for anticipating the broader patterns of climate-induced change to permafrost terrain, and the subsequent identification of areas deemed to be particularly sensitive (mainly in an engineering context) to continued atmospheric warming.

However, considerably more detailed information is needed to support route selection and/or route evaluation activities in conjunction with the construction of proposed new pipelines and highways in the Mackenzie River valley. To that end we have begun compilation of a high-resolution (30 m) database for the Mackenzie valley in partnership with the Forest Management Branch of the GNWT Department of Resources, Wildlife and Economic Development (RWED). The database will enable spatial modeling at a level of detail compatible with the scale of operations of most engineering projects, particularly pipelines and roads. It is expected that high-resolution ground thermal modeling can support informed decision-making and sound planning for future engineering projects, and thereby contribute to the long-term stability of man-made structures in a changing permafrost landscape. The GSC modeling group has developed a working arrangement and the GNWT Department of Transport that should afford the opportunity to test our ground thermal model in conjunction with an actual highways development project sometime during the next 2-3 years.

Compilation of a high-resolution spatial database supporting detailed geothermal modeling within the so-called Mackenzie Valley Transportation Corridor is well underway. This dataset is keyed to the 30m resolution of Landsat-derived satellite imagery, and includes:

1. Digitized versions of the Environmental Social Program Map Series 101 entitled “Vegetation Types of the Mackenzie Valley Corridor” (CFS, 1974), based on the interpretation of aerial photographs (approx. 30 map sheets).

2. An Enhanced Vegetation Classification (EVC) integrates a Landsat-derived vegetation classification (30m) produced by the RWED, with forest species information from the ESP Map Series 101.

3. Digital versions of 1:125,000 surficial geology maps intersecting the Mackenzie Valley Transportation Corridor (approx. 34 map sheets).

4. High-resolution digital elevation model derived from 1:50,000 NTDB base maps for selected areas.

Landsat derived vegetation classification

The core element of the high resolution database is a 30m Landsat-derived vegetation cover classification being produced by the Forest Management Branch of the RWED and subsequently enhanced by the GSC through integration of forest species information from existing polygon maps (1:125,000) of vegetation cover in the Mackenzie Transportation corridor (Environmental Social Program, 1974). To date 8 images have been received, covering approximately 50% of the so-called Mackenzie Transportation Corridor (Figure 17). The RWED classifications provided are preliminary, with final versions (including a statistical evaluation of classification accuracy) requiring another year or so for completion. In the broader context, the development of a comprehensive, database (of surficial geology, vegetation cover, digital elevation data,), supporting high-resolution ground thermal modeling within the entire Mackenzie Trasnsportation Corridor has been undertaken, but will require 2-3 more years for completion. We have selected two areas in the vicinity of Fort Simpson and Norman Wells as demonstration sites for high-resolution modeling. In addition to high-resolution satellite imagery, the modeling employed relatively detailed 1:125,00 surficial geology maps and digital elevation models derived through interpolation of NTS contour maps (1:50,000 and 1:250,000 for Fort Simpson and Norman Wells respectively). The assignment of model parameter values (n-factors, soil bulk density, water content, thermal conductivity) was based on the information presented in Tables 1 and 2. Values for DDF and DDT for the two study areas were based on climate data collected at the Fort Simson and Norman wells airports.

5.3.1 An Enhanced Vegetation Classification (EVC)

An example of the Enhanced Vegetation Classification produced for the Fort Simpson area is presented in Figure 18. This classification was generated through integration of ancillary information about the dominant tree species occurring in individual forest stands (ESP Map Series 101) and the 30m resolution Landsat-derived vegetation classification (preliminary) produced by RWED. The EVC retains the high level of spatial discrimination inherent to Landsat imagery, but has the advantage of enhanced thematic discrimination not currently achievable in satellite-based classifications, primarily with respect to identification of the dominant conifer species in forest stands (i.e. black spruce, white spruce and pine). These distinctions are very important in terms of the establishment of appropriate values for model input parameters (n-factors, saturation ratio), especially as each of these species tends to be associated with different soil moisture conditions. Note that it is only possible to produce an Enhanced Vegetation Classification in areas of overlap between the satellite imagery and the ESP map data (shown in Figure 17).

The Enhanced Vegetation Classification produced for the Norman Wells study area is presented in Figure 19. Although derived in a similar fashion, the class descriptions are not precisely identical to those of the Fort Simpson EVC, due to differences in the

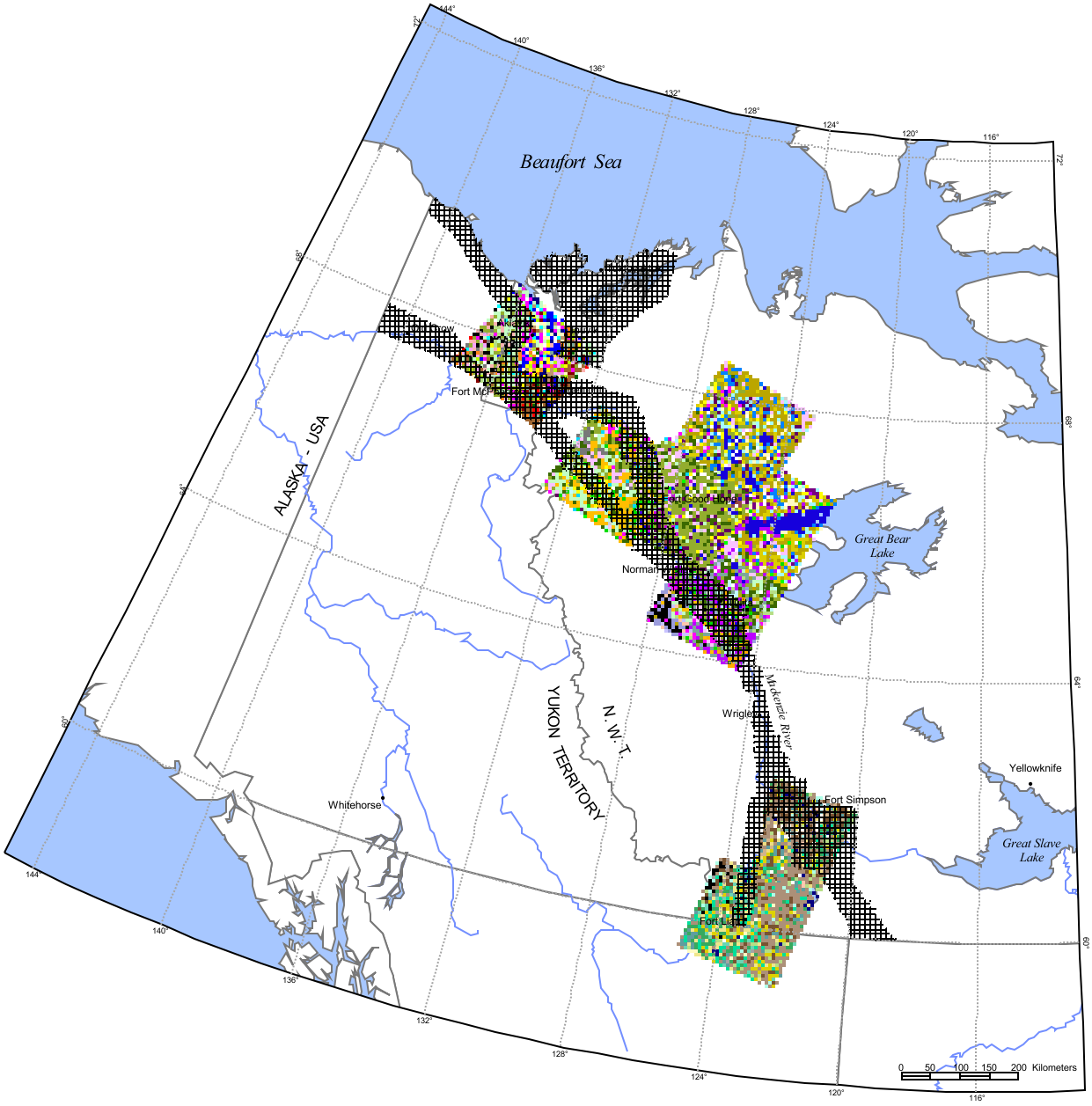

Satellite imagery coverage to date for the Mackenzie River Valley Transportation Corridor (showned in hatch pattern).

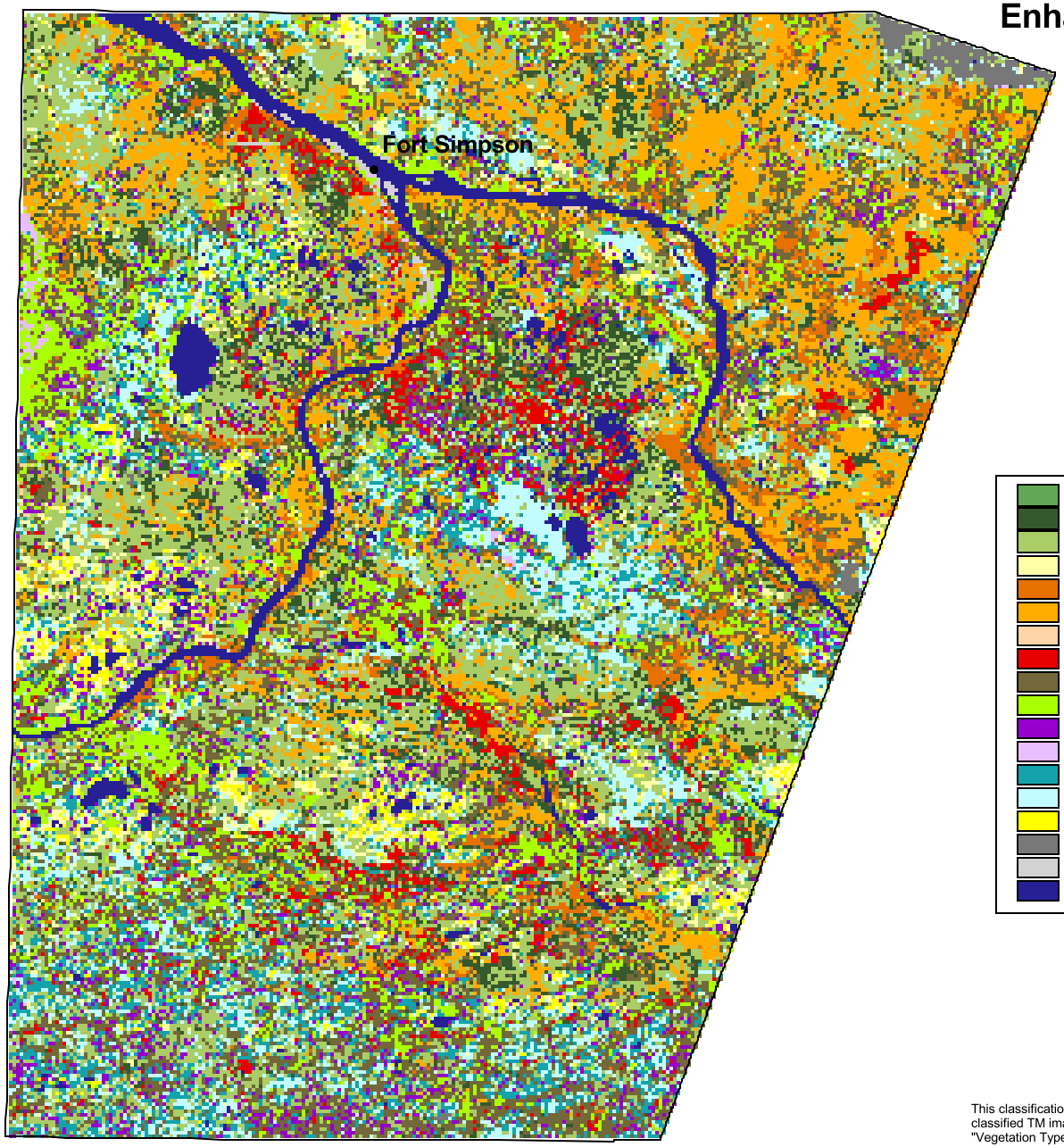

Enhanced Vegetation Classification
Fort Simpson, NWT

N
W
E
S

- Dense Conifer Forest (U)
- Dense Black Spruce
- Open Stunted Black Spruce Transitional Forest
- Black Spruce Lichen Transitional Forest
- Dense White Spruce
- White Spruce - Feathermoss
- White Spruce (riparian)
- Pine Dominant
- Close canopy mix forest
- Deciduous
- Open Tree Shrub Mixture
- Upland / Riparian Shrubs
- Wetland Shrubs
- Fen / Wet Sedges
- Sphagnum (Lichen)
- Older Burn with Early Regeneration
- Bare / Developed / Sparse
- Water

0 5 10 15 20 25 Km

This classification was produced by the Geological Survey of Canada through integration of classified TM imagery (GNWT, 1996) and the Environmental Social Program map series "Vegetation Types of the Mackenzie Corridor" (Canadian Forest Service, 1974).

Figure 18

Enhanced Vegetation Classification
Norman Wells, NWT

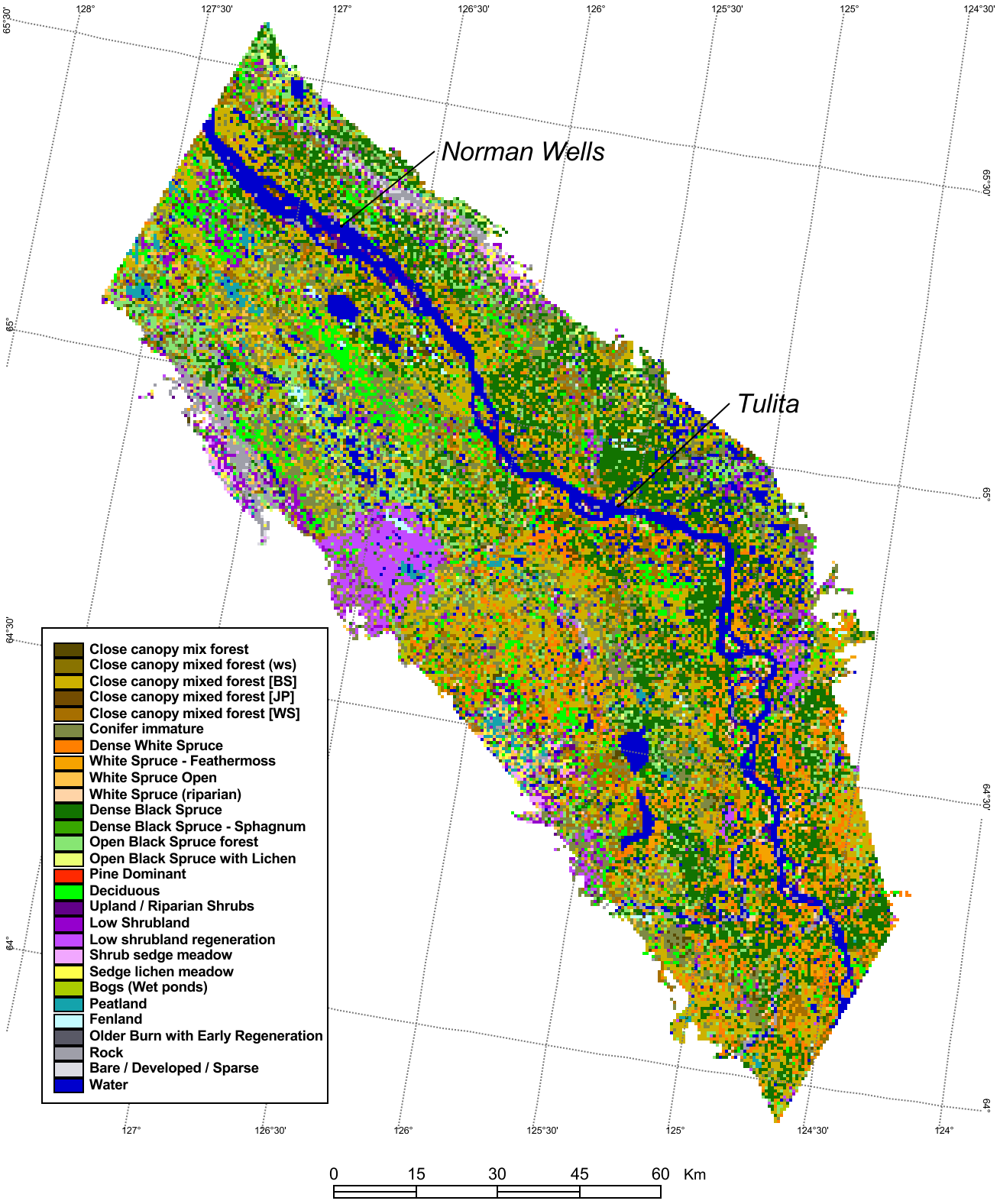

preliminary Landsat-based vegetation classifications provided by RWED. Because at present we have only a limited set of n-factor values representing different vegetation cover types, the EVCs contains more detail (primarily in terms of the composition of mixed forests) than was actually employed in the modeling.

5.3.2 Results of high-resolution spatial modeling

Norman Wells

Figure 20 presents TTOP predictions of the distribution and thickness of permafrost in the vicinity of Norman Wells, under the baseline climate scenario (MAAT = -6°C). The results suggest that permafrost underlies about 84% of terrain in the Norman Wells study area (Table 7), while 16% of terrain is permafrost free. Permafrost is generally widespread at Norman Wells, with permafrost of greater than 10 m in thickness extending over 78% of terrain, as compared to about 9% at Fort Simpson (Table 8).

Figure 21 presents model predictions of the equilibrium distribution of permafrost at Norman Wells following an increase in mean annual air temperatures of 1C°. A comparison of the predicted extent of permafrost to that of the baseline climate scenario (Table 7) suggests that permafrost thickness will decrease substantially throughout the Norman Wells region in response to a very modest atmospheric warming, while the overall extent of permafrost will decrease only moderately (to about 74% of the study area, as compared to 84 % under the baseline climate scenario).

Table 7: Model predictions of the areal extent of permafrost in the Norman Wells region.

MAAT: -6°C (baseline climate)			
Class	Description	Percent	Frozen
1	Unfrozen	16.13	83.87
2	0-10m	5.51	
3	10-20m	23.54	
4	20-30m	43.24	
6	>30m	11.58	
		100	
MAAT: -5°C (1°C atmospheric warming)			
Class	Description	Percent	Frozen
1	Unfrozen	25.68	74.33
2	0-10m	24.06	
3	10-20m	43.00	
4	20-30m	7.12	
5	>30m	0.14	
		100	

Fort Simpson

The high-resolution modeling predictions for the distribution and thickness of permafrost in the vicinity of Fort Simpson are presented in Figure 22. Under the baseline climate

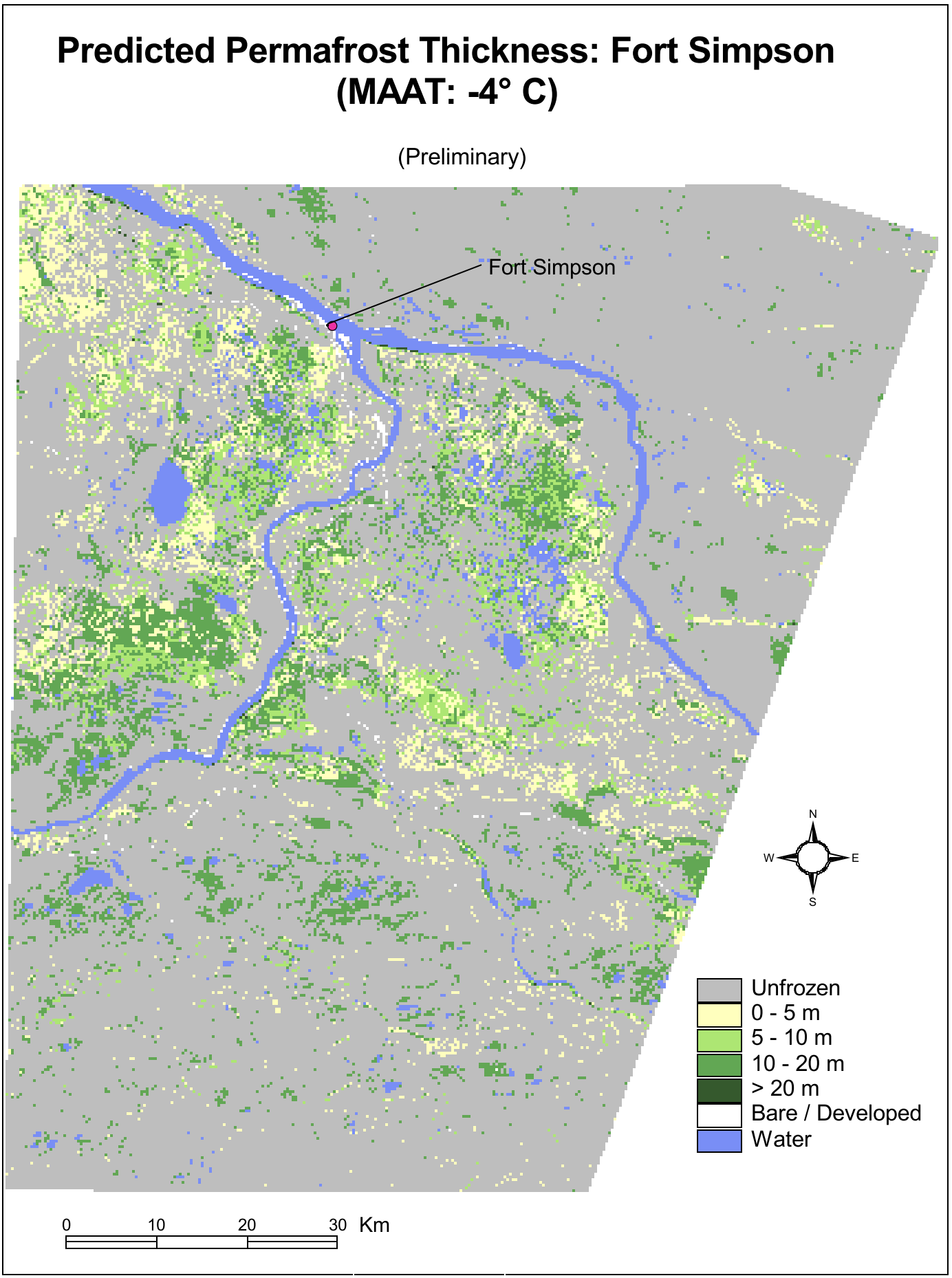
Predicted Permafrost Thickness: Fort Simpson
(MAAT: -4° C)
(Preliminary)
Fort Simpson
N
W
E
S
Unfrozen
0 - 5 m
5 - 10 m
10 - 20 m
> 20 m
Bare / Developed
Water
0
10
20
30
Km

Predicted permafrost thickness under three climate scenarios: Fort Simpson

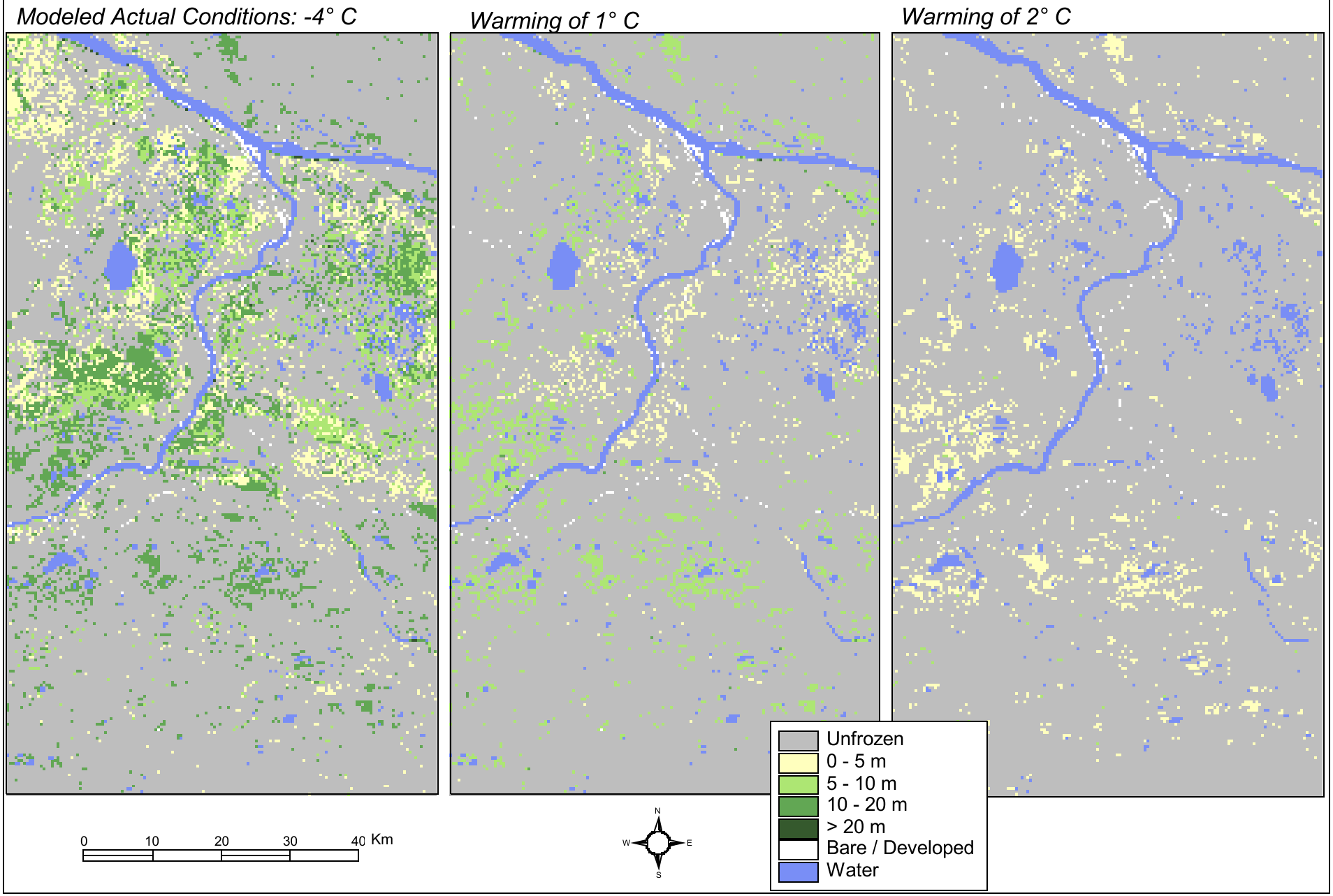

Figure 21

scenario (MAAT: - 4°C) the modeling suggests that 21% of the study area is underlain by permafrost, with the bulk of that occurring in lowland areas proximate to the confluence of the Liard and Mackenzie rivers (although the areal extent of permafrost may be as high as 34% locally). Most of the permafrost is predicted to be between 5 and 20 m in thickness (Table 8) although the model predicts the occurrence of thin permafrost (< 5m in thickness) over about 7% of the region. Recall that confidence is relatively low for this class of "marginal" permafrost, and we should consider that within this category, permafrost may or may not actually be present at any given location. The model predicts that less than 1% of the Fort Simpson area is underlain by permafrost of greater than 20m thickness, compared to about 55% at Norman Wells.

Table 8: Model predictions of the areal extent of permafrost in the Fort Simpson region.

MAAT: -4C (baseline climate)			
Class	Description	Percent	Frozen
1	Unfrozen	78.95	21.05
2	0-5m	7.03	
3	5-10m	4.86	
4	10-20m	9.103	
5	>20m	0.06	
		100	
MAAT: -3C (1°C atmospheric warming)			
Class	Description	Percent	Frozen
1	Unfrozen	92.86	7.14
2	0-5m	2.26	
3	5-10m	4.78	
4	10-20m	0.096	
5	>20m	0.00	
		100	

Model predictions of the distribution and thickness of permafrost in the Fort Simpson area under two scenarios of climate warming (1 & 2°C increases in MAAT) are presented in Figure 23 (the modeling assumes that thermal equilibrium has been re-established following warming). Under the 1°C warming scenario (MAAT = -3°C), the portion of the study area underlain by permafrost decreased to about 7%, nearly all of which is less than 10 m in thickness. Following a further 1°C warming (MAAT = -2°C) , the areal extent of permafrost is predicted to decrease to less than 5% of the study area, essentially persisting only in association with raised peat bog features (peat plateaus). Note that these predictions are generally consistent (both statistically and spatially) with the results of low-resolution modeling of the Fort Simpson area under an atmospheric warming of 2 Celcius degrees.

5.4 Prospectus for Route Evaluation/Route selection

The major objectives of this project were the realization of a regional-scaled ground thermal modeling capability and the compilation of comprehensive spatial databases

Predicted Permafrost Thickness (MAAT: -6° C) : Region of Norman Wells and Tulita

(Preliminary)

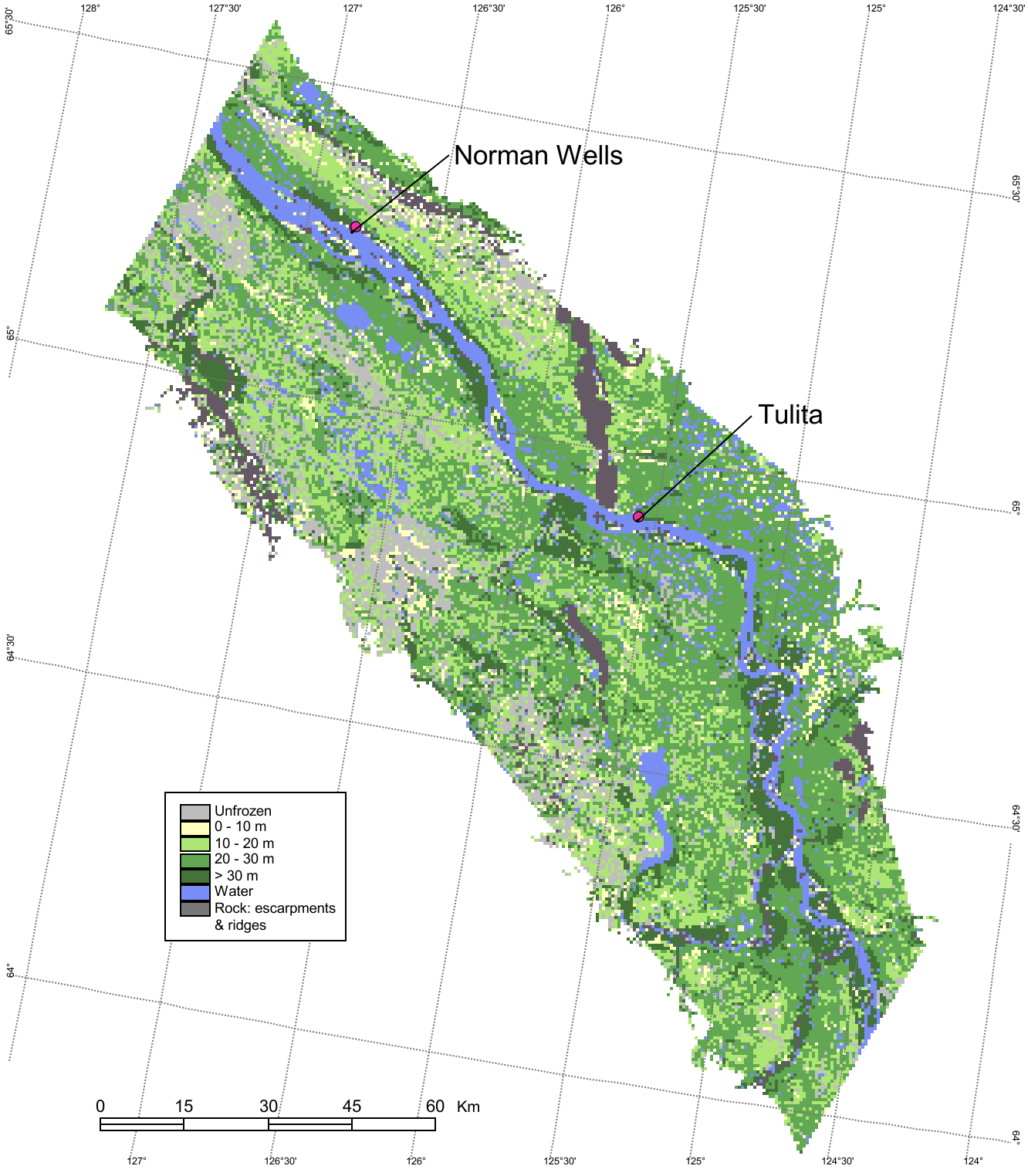

Predicted Permafrost Thickness (MAAT: -5° C) : Region of Norman Wells and Tulita

(Preliminary)

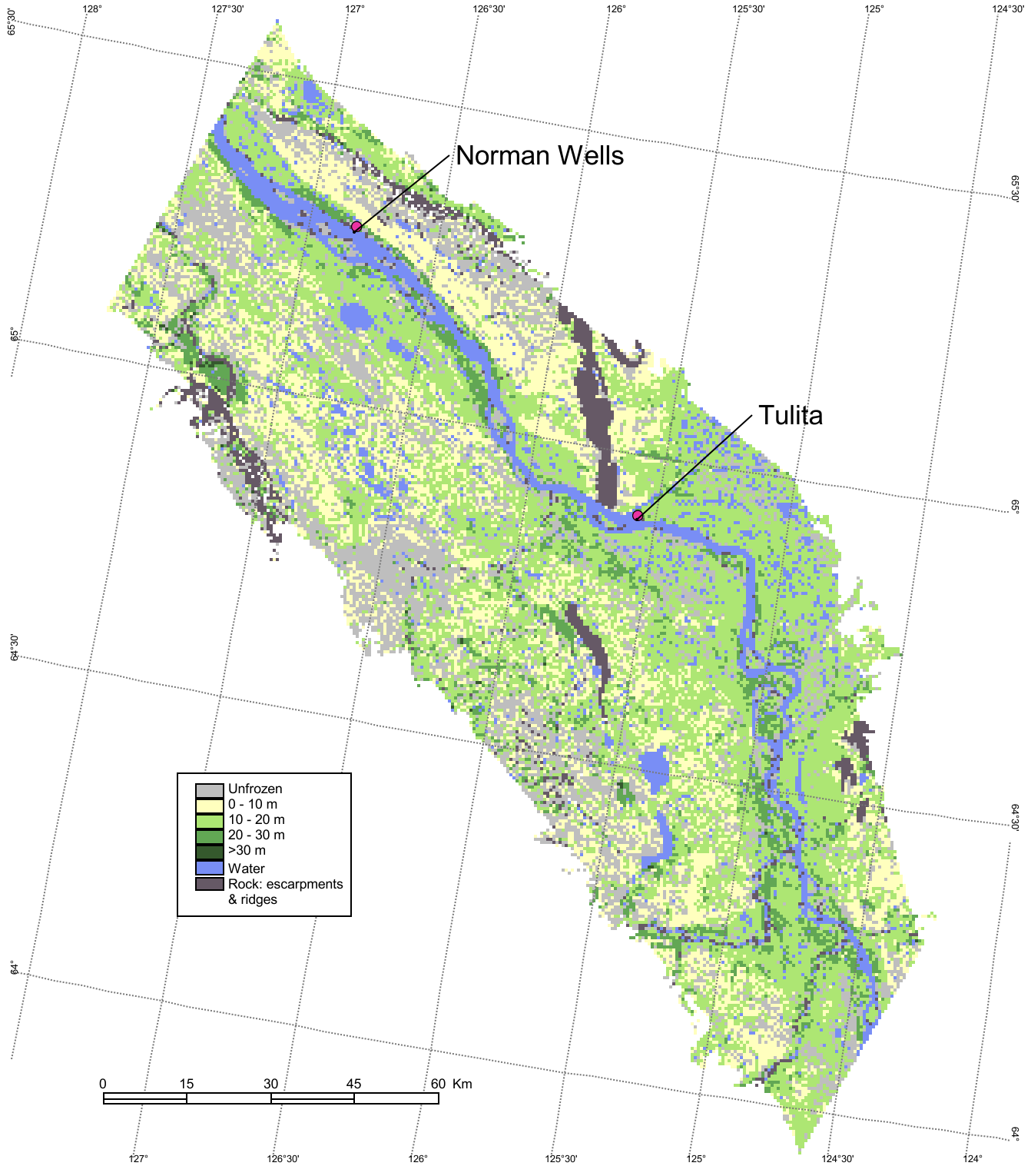

supporting route selection and route evaluation applications in the Mackenzie Valley Transportation Corridor, in anticipation of planned new pipeline and highway development during the next few decades. This is a very substantial undertaking, and while progress has been very satisfactory to date, some aspects of the work are expected to continue for several more years, particularly with respect to completion of the spatial databases. This situation was anticipated and was explicitly identified as a project constraint at the project proposal stage.

Decision-making for route selection and route evaluation applications depends upon access to reliable, suitably-scaled data about local-regional terrain conditions. In northern regions, this must include an understanding of ground thermal conditions (i.e. the distribution of permafrost) and associated terrain sensitivity in the face of progressive climate warming. Given that such information is not available directly (in the form of readily-available, suitably-scaled maps), we must adopt appropriate techniques for predicting the likely distribution of frozen ground. Numeric modeling provides a means for conducting rigorous assessments of the potential impacts of climate change on permafrost landscapes. A detailed assessment is beyond the scope of this report, however we do present the results of a simple evaluation of the existing highway right-of-way in the vicinity of Fort Simpson, N.T. (Figure 24) which identifies points of intersection between the right-of-way and terrain for which the presence of permafrost (greater than 5m in thickness) is likely. As a cursory example of the utility of both the spatial databases and the ground thermal model developed under this project, this map identifies sections of the highway that may require special attention with respect to maintenance requirements over the next several decades.

Table 9: Intersection of highways in the Fort Simpson region with permafrost terrain

Permafrost class	Map area (%)	Intersection (%)	
		Road path	12 km corridor
Unfrozen	78.95	80.64	69.93
0 to 5 m	7.03	6.52	8.06
5 to 10 m	4.86	4.26	5.45
10 to 20 m	9.10	7.87	16.06
> 20 m	0.06	0.71	0.49
Total	100.00	100.00	100.00

Table 9 compares the overall areal extent of permafrost within the Fort Simpson study area to the proportion of the highway intersecting permafrost bearing terrain (as predicted by the TTOP ground thermal model). It is interesting to note that the statistics for the permafrost extent within the study area and the figures for the actual road path intersection with permafrost terrain are almost identical, suggesting that there was effectively no avoidance of permafrost in the original route selection for the highway. However, when we analyze the terrain within 6 km either side of the highway we discover that a significant increase in extent of permafrost within this corridor (about 30% of terrain as compared to 20% regionally). On this basis we can conclude that the highway right-of-way does in fact avoid permafrost terrain locally, although we have no

Intersection of the existing highway with TTOP prediction of permafrost in the vicinity of Fort Simpson

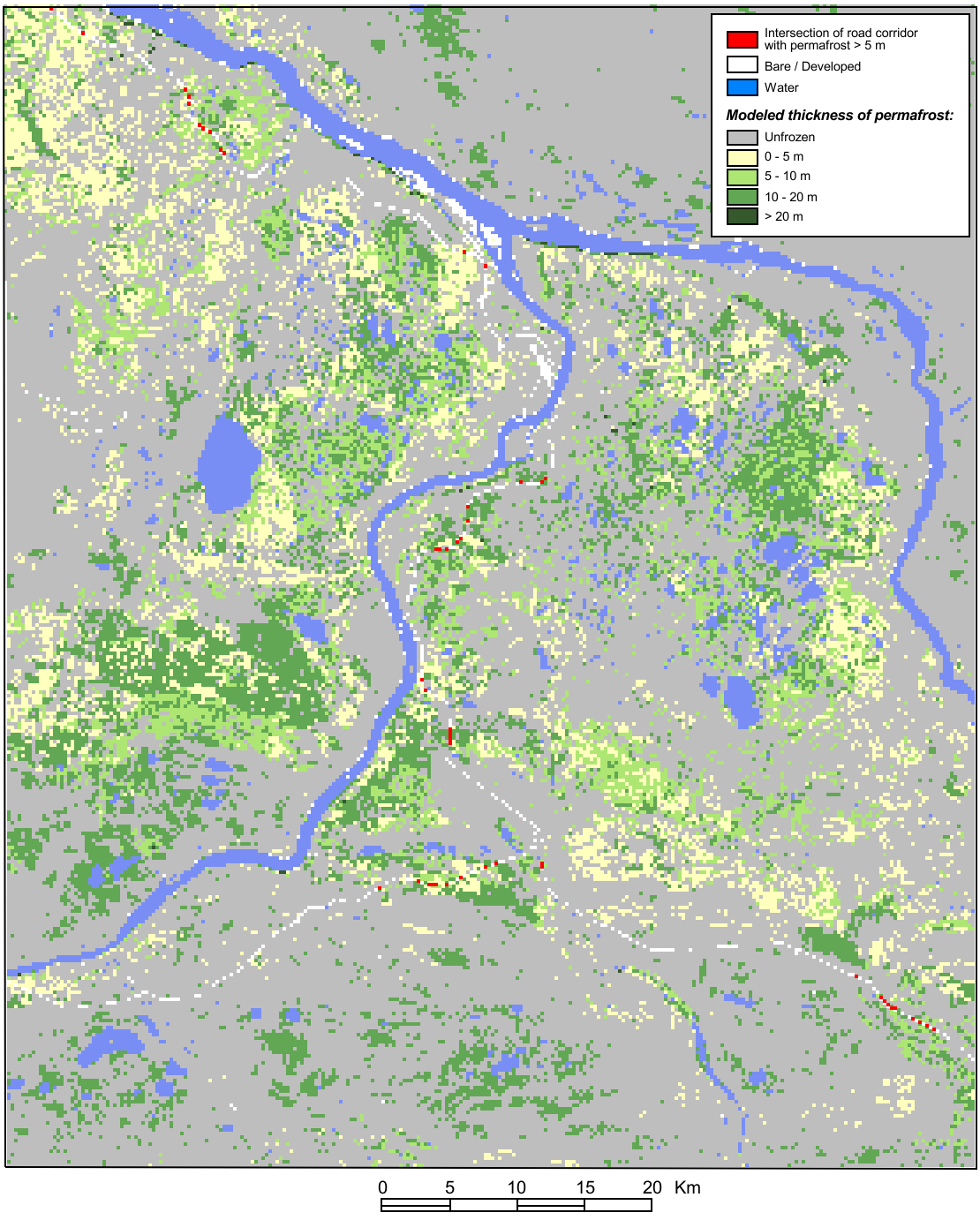

indication that this was a specific criterion considered during the original selection of the highway route.

6 SUMMARY

A simple numeric relation (TTOP) has been shown to provide estimates of the equilibrium temperature at the top of permafrost that are nearly identical to those generated by sophisticated finite-element methods. A set of model parameter values representing the dominant climate and terrain factors influencing the ground thermal regime in the Mackenzie River valley was established by optimizing the performance of the TTOP model (in terms of correctly predicting the presence/absence of permafrost) within a dataset of 154 geotechnical boreholes located along the Norman Wells Pipeline right-of-way. These parameter values were assumed to be transferable to the broader Mackenzie valley, given that the range of terrain conditions encountered at borehole sites are generally representative of the surficial geology and vegetation cover types in the broader region.

Satellite imagery, conventional map data, and regional digital elevation models provide information about terrain conditions in the Mackenzie River valley, which serve as a basis for the determination of appropriate parameter values for spatial modeling of ground thermal conditions. Low-resolution modeling of the entire Mackenzie River valley (north of 60°N) and high-resolution modeling in the vicinity of Fort Simpson and Norman Wells was undertaken using ArcView® and ArcInfo® Geogrphic Information Systems. A series of maps were produced depicting the estimated distribution of permafrost (in terms of occurrence and thickness) under prevailing climate conditions and in response to a number of climate warming scenarios. An index of terrain sensitivity to climate change was also produced, which accounts for both the predicted thermal responses and potential physical responses of terrain to sustained atmospheric warming.

Because the TTOP relation is constrained by the assumption that thermal equilibrium has been achieved between the atmospheric and ground thermal regimes, the model provides no indication of the time required to realize the changes predicted. A new 3-year PERD project has been approved to investigate transient (time-dependent) aspects of climate change in the Mackenzie Valley. This project will complement a concurrent GSC project to conduct a comprehensive assessment of the sensitivity of Mackenzie Valley terrain to climate warming, by providing time frames within which we may anticipate thermal and physical disturbance of the landscape.

Acknowledgments:

Major funding for this project was provided by the Climate Change Action Fund (CCAF) and the Panel on Energy Research and Development (PERD). The GSC also wishes to thank the Government of the Northwest Territories Department of Resources, Wildlife, and Economic Development (RWED) and the Department of Transportation (DOT) for their enthusiatic participation and their very significant contribution to this work.

References:

Aylsworth, J.M., Burgess, M.M., Desrochers, D.T., Duk-Rodkin, A., Robertson, T., and J.A. Tranor (2000). Surficial Geology, subsurface materials, and thaw sensitivity of sediments. in *The Physical Environment of the Mackenzie Valley, Northwest Territories: ABaseline for the Assessment of Environmental Change.* L.D. Dyke and G.R. Brooks (Ed.) GSC Bulletin 547, 2000. 208 p. 41-78.

Aylsworth, J.M., and I.M. Kettles (2000) Distribution of peatlands. in *The Physical Environment of the Mackenzie Valley, Northwest Territories: ABaseline for the Assessment of Environmental Change*. L.D. Dyke and G.R. Brooks (Ed.) GSC Bulletin 547, 2000. p. 49-55.

Canada Centre for Remote Sensing (1999). *Land Cover of Canada.* MCR0103.

Environment Canada, (1982) *Canadian Climate Normals (Temperature) 1951-80.* Volume 2, 306 pages.

Environment Canada, (1982) *Canadian Climate Normals (Degree-days) 1951-80.* Volume 4, 280 pages.

Environment Canada, (1975) *Canadian Climate Normals (Precipitation) 1941-70.* Volume 2-SI, 333 pages.

Environmental Social Program, (1974). Vegetation Types of the Mackenzie Corridor. *Task Force on Northern Oil Development*, Report No. 73-46, 85 pages.

Farouki, O.T., (1981). Thermal properties of soils; U.S. Army Cold Regions Research and Engineering Laboratory , *CCREL Monograph No. 81-1*, 136 pages.

Goodrich, L.E. (1978). Some results of a numerical study of ground thermal regimes, In *Third International Conference on Permafrost*, Edmonton, Canada. pp. 30-34

Goodrich, L.E. (1982). *An introductory review of numerical methods for ground thermal regime calculations.* Division of Building Research, National Research Council of Canada, DBR Paper No. 106, 133 pages.

Hegginbottom, J.A., Dubreuil, M.A., and P.T. Harker (1995) Canada, Permafrost. in *National Atlas of Canada.* 5th ed. National Atlas Information Centre, Natural Resources Canada, MCR 4177, scale: 1:7,500,000.

Hinkle, K.E. and S.I. Outcalt (1994) Identification of heat transfer processes during soil cooling, freezing, and thawing in Central Alaska. *Permafrost and Periglacial Processes*, **5**, pp 217-235.

Interprovincial Pipe Lines (NW) Ltd. (1982a). *Norman Wells Pipeline Project 1982 Drilling Program Data Report* (unpublished). IPL, Edmonton, Canada.

Interprovincial Pipe Lines (NW) Ltd. (1982b). Norman Wells Pipeline Project - Delineation of Permafrost Distribution by Geophysical Survey. Summary Report KMP 0 to 868.3, December 1982: Report to the National Energy Board of Canada.

Johansen, O. (1975). *Thermal conductivity of soils*. Ph.D. Thesis, Trondheim, Norway. (CRREL Draft Translation 637, 1977, AD044002).

Jorgenson, M.T. and R.A. Kreig (1988). A model for mapping permafrost distribution based on landscape component maps and climatic variables. *Proceedings, Fifth International Conference on Permafrost,* Vol. 1, Trondheim, Norway, pp. 176-82.

Judge, A.S. (1973). Thermal regime of the Mackenzie Valley: observations of the natural state. Report 37-38, *Environmental Social Committee, Northern Pipelines, Task Force on Northern Oil Development*, Government of Canada (177 pp.).

Judge, A.S. (1975). *Geothermal studies in the Mackenzie Valley by the Earth Physics Branch*. Geothermal Service of Canada, Earth Physics Branch, Energy Mines and Resources Canada, Geothermal Series No. 2 (12 pp.).

Lee, R. (1964). *Potential insolation as a topoclimatic characteristic of drainage basins*. International Association of Science in Hydrology Bulletin 1133 (121 pp.).

Lunardini, V.J. (1981). *Heat Transfer in Cold Climates*. Van Nostrand Reinhold Company, Toronto (731 pp.).

Luthin, J. N. and Guymon, G.L. (1974*).* Soil moisture-vegetation-temperature

relationships in central Alaska. *Journal of Hydrology*. 23. pp 233-246.

Outcalt, S.I., Nelson, F.E. and K.E. Hinkle (1990). The zero curtain effect: heat and mass transfer across an isothermal region in freezing soil. *Water Resources Research.* 26. 1509-1516.

Pilon J., Burgess M., Judge, A., Allen, V., MacInnes K., Harry D., Tarnocai, C., and H. Baker (1989), *Norman Wells to Zama Oil Pipeline permafrost and terrain research and monitoring program: site establishment report*. Geological Survey of Canada Open File Report No. 2044 (331 pp.).

Smith, M.W., and D.W. Riseborough (1996). Permafrost Monitoring and Detection of Climate Change, *Permafrost and Periglacial Processes*, **7**, 301-309.

Smith, S. and M.M. Burgess (2000). Ground Temperature Database for Northern Canada. Geological Survey of Canada Open File Report No. 3954. 28 pages.

Taylor, Alan E. (1995). Field measurements of n-factors for natural forest areas, Makenzie Valley, Northwest Territories. *Current Research* 1995-B. Geological Survey of Canada (pp. 89-98).

Wright, J.F. (1995). *A Hybrid Model for Predicting Permafrost Occurrence and Thickness*. Unpublished MA Thesis, Carleton University, Ottawa, Canada (80 pp.).

APPENDIX 1

Status of specific tasks associated with CCAF Project A073

Item	Task Description	Status	Comment
1	Digitizing of ESP vegetation maps for the Wrigley and Fort Good Hope regions.	C	Series of 60 ESP maps (1:125,000) have been digitized covering the entire Mackenzie Corridor.
2	Parameterization of model variables and production of preliminary maps showing predicted permafrost distribution and thickness under the current climate at Wrigley and Fort Good Hope, using ESP vegetation data.	C,M	Modeling in Wrigley and Fort Good Hope areas abandoned due to data quality & availability issues. Model parameters have been established for alternative study regions at Fort Simpson and Norman Wells.
3	Acquisition and integration of Landsat vegetation classification for Norman Wells and Wrigley regions.	C,M	GNWT satellite imagery not yet available for the Wrigley region. Norman wells complete.
4	Development of a model component for predicting active-layer thickness.	C	A simple phase change solution was adopted. Model tends to systematically overestimate active layer thickness.
5	Acquisition and integration of classified Landsat imagery for the Fort Good Hope region.	I	Satellite imagery obtained but preliminary GNWT classification deemed unreliable.
6	Produce maps for the selected regions predicting the characteristics of permafrost under the current climate regime and for various scenarios of climate warming.	C	High resolution (30m)maps depicting model predictions of permafrost distribution in the Fort Simpson and Norman Wells regions.
7	Produce preliminary low-resolution maps predicting changes to permafrost and associated impacts within the greater Mackenzie Valley, under various scenarios of climate warming.	C	1 km resolution maps depicting model predictions of permafrost distribution in the Mackenzie valley and potential responses to increases in mean annual air temperature of 2°C and 5°C.
8	Summary Report outlining the development of relevant spatial datasets, the institution of the modeling approach, and model predictions of the impacts of climate change on permafrost in the Mackenzie valley Corridor.	C	Emphasis has been placed on reporting the results of modeling at the broad regional scale. Work on the high resolution modeling component will continue over the next few years.

Note: C = Complete, I = Incomplete, M = modified

APPENDIX 2
154 Geotechnical boreholes - IPL 1982

Record #	*Borehole*	*KP*	*Terrain*	*Soil*	*Vegetation*	*Texture*	*Dry Density*	*Saturation (%)*	*Nt*	*Nf*	*Kt*	*Kf*	*MAAT*	*T_TOP*	*Predicted*	*Observed*	*Mode*	*Predicted Depth*
1	82-s19b	270.797	Colluvium	clay	B.Spruce	1	1440	0.85	0.60	0.24	1.21	1.92	-5.1	-0.53	F	F	1	25.18
2	82-s19c	270.797	Colluvium	clay	B.Spruce	1	1440	0.85	0.60	0.24	1.21	1.92	-5.1	-0.53	F	F	1	25.18
3	82-s20a	270.797	Colluvium	clay	Spruce	1	1440	0.80	0.80	0.31	1.18	1.81	-5.08	-0.52	F	F	1	23.74
4	82-s20b	270.797	Colluvium	sand	Spruce	2	1440	0.80	0.80	0.31	1.53	2.44	-5.1	-0.62	F	F	1	37.49
5	82-s20c	270.797	Colluvium	clay	Spruce	1	1440	0.80	0.80	0.31	1.18	1.81	-5.1	-0.52	F	F	1	23.74
6	82-s21a	272.825	Colluvium	clay	Spruce	1	1440	0.80	0.80	0.31	1.18	1.81	-5.1	-0.52	F	F	1	23.58
7	82-s21b	273.080	Colluvium	clay	B.Spruce	1	1440	0.85	0.60	0.24	1.21	1.92	-5.1	-0.52	F	F	1	25.04
8	82-s22a	273.080	Colluvium	clay	B.Spruce	1	1440	0.85	0.60	0.24	1.21	1.92	-5.1	-0.52	F	F	1	25.04
9	82-s22b	273.080	Colluvium	clay	B.Spruce	1	1440	0.85	0.60	0.24	1.21	1.92	-5.1	-0.52	F	F	1	25.04
10	80-42	274.990	Lacustrine	clay	Spruce-Tamarac	1	1500	0.80	0.80	0.31	1.22	1.83	-5.1	-0.45	F	F	1	20.47
11	82-105	274.990	Lacustrine	clay	B.Spruce	1	1500	0.85	0.60	0.24	1.25	1.93	-5.1	-0.47	F	F	1	22.68
12	82-s23c	277.980	Colluvium	clay	W.Spruce	1	1440	0.80	0.80	0.31	1.18	1.81	-5.0	-0.51	F	F	1	23.19
13	82-s26a	285.123	Colluvium	gravel/clay	Poplar	2	1440	0.55	0.90	0.30	1.37	1.74	-5.0	0.69	U	U	1	0.00
14	82-s26b	285.123	Colluvium	clay	Poplar	1	1440	0.55	0.90	0.30	1.26	1.63	-5.0	0.60	U	U	1	0.00
15	82-s26c	285.123	Colluvium	clay	Poplar	1	1440	0.55	0.90	0.30	1.26	1.63	-5.0	0.60	U	U	1	0.00
16	82-s27b	286.267	Colluvium	clay	B.Spruce	1	1440	0.85	0.60	0.24	1.21	1.92	-5.0	-0.51	F	F	1	24.25
17	82-111	286.687	Lacustrine	peat/clay	B&W Spruce	1	1500	0.85	0.60	0.24	1.25	1.93	-5.0	-0.46	F	F	1	21.97
18	82-109	286.687	Lacustrine	clay	B.Spruce	1	1500	0.85	0.60	0.24	1.25	1.93	-5.0	-0.46	F	F	1	21.97
19	81-110	286.687	Lacustrine	clay	B.Spruce	1	1500	0.85	0.60	0.24	1.25	1.93	-5.0	-0.46	F	F	1	21.97
20	80-46	288.950	Lacustrine	clay	B.Spruce	1	1500	0.85	0.60	0.24	1.25	1.93	-5.0	-0.45	F	F	1	21.83
21	82-112	291.561	Lacustrine	clay	B.Spruce	1	1500	0.85	0.60	0.24	1.25	1.93	-5.0	-0.45	F	F	1	21.67
22	82-134	298.383	Alluvial	gravel-sand	Pine	2	1600	0.50	0.80	0.35	1.49	1.68	-5.0	0.10	U	U	1	0.00
23	82-113	298.383	Alluvial	gravel	Pine	2	1600	0.50	0.80	0.35	1.49	1.68	-5.0	0.10	U	U	1	0.00
24	80-49	300.466	Lacustrine	clay	Spruce	1	1500	0.80	0.80	0.31	1.22	1.83	-5.0	-0.40	F	F	1	18.49
25	82-139	304.866	Alluvial	sand	Spruce-Birch	2	1600	0.70	0.85	0.31	1.66	2.25	-4.9	0.09	U	U	1	0.00
26	82-135	307.000	Lacustrine	silt	Spruce	1	1500	0.80	0.80	0.31	1.22	1.83	-4.9	-0.39	F	F	1	17.98
27	80-51	307.943	Lacustrine	clay	B.Spruce	1	1500	0.85	0.60	0.24	1.25	1.93	-4.9	-0.43	F	F	1	20.66
28	82-136	315.343	Lacustrine	clay/sand	Pine	1	1500	0.50	0.80	0.35	1.25	1.53	-4.9	-0.18	F	F	1	6.73
29	82-137	315.343	Lacustrine	silt	Spruce	1	1500	0.80	0.80	0.31	1.22	1.83	-4.9	-0.38	F	F	1	17.33

Record #	Borehole	KP	Terrain	Soil	Vegetation	Texture	Dry Density	Saturation (%)	Nt	Nf	Kt	Kf	MAAT	T_TOP	Predicted	Observed	Mode	Predicted Depth
30	82-138	315.343	Lacustrine	clay	B.Spruce	1	1500	0.85	0.60	0.24	1.25	1.93	-4.9	-0.42	F	F	1	20.21
31	82-s30a	324.179	Colluvium	clay	B.Spruce	1	1440	0.85	0.60	0.24	1.21	1.92	-4.9	-0.46	F	F	1	21.98
32	82-s30b	324.179	Colluvium	sand	B.Spruce	2	1440	0.85	0.60	0.24	1.56	2.58	-4.9	-0.54	F	F	1	34.98
33	82-89	325.020	Lacustrine	clay/sand	B.Spruce	1	1500	0.85	0.60	0.24	1.25	1.93	-4.9	-0.41	F	F	1	19.62
34	82-88	325.871	Lacustrine	sand	B.Spruce	2	1500	0.85	0.60	0.24	1.63	2.61	-4.8	-0.49	F	F	1	31.71
35	82-91	330.061	Glaciofluvial	silt	B.Spruce-Poplar	1	1550	0.85	0.60	0.24	1.29	1.94	-4.8	-0.36	F	F	1	17.30
36	82-92	333.694	Till	clay	Poplar-Spruce	1	1750	0.55	0.90	0.30	1.59	1.82	-4.8	1.18	U	F	0	0.00
37	82-114	339.513	Glaciofluvial	gravel	Pine	2	1550	0.50	0.80	0.35	1.44	1.65	-4.8	0.11	U	U	1	0.00
38	82-93	341.148	Till	silt/sand	B.Spruce	1	1750	0.85	0.60	0.24	1.45	2.00	-4.8	-0.16	F	F	1	7.82
39	82-115	343.945	Till	sand/clay	B.Spruce-Pine	2	1750	0.85	0.60	0.24	1.95	2.77	-4.8	-0.21	F	F	1	14.73
40	82-113	345.937	Till	sand/silt	B.Spruce	2	1750	0.85	0.60	0.24	1.95	2.77	-4.8	-0.21	F	F	1	14.54
41	80-58	346.662	Till	clay	B.Spruce	1	1750	0.85	0.60	0.24	1.45	2.00	-4.8	-0.15	F	U	0	7.45
42	80-59	346.662	Till	clay	B.Spruce	1	1750	0.85	0.60	0.24	1.45	2.00	-4.8	-0.15	F	U	0	7.45
43	81-s40b	350.899	Lacustrine	clay/silt	Birch-Spruce	1	1500	0.70	0.80	0.35	1.47	2.06	-4.7	-0.53	F	F	1	27.28
44	81-s40a	350.899	Colluvium	clay-silt	Spruce-Birch	1	1440	0.70	0.85	0.31	1.12	1.61	-4.7	-0.04	F	F	1	1.51
45	82-47	353.449	Till	silt	W.Birch	1	1750	0.70	0.80	0.35	1.77	2.23	-4.7	-0.19	F	F	1	10.86
46	82-49	353.449	Till	gravel/clay	Pine	2	1750	0.50	0.80	0.35	1.67	1.76	-4.7	0.48	U	U	1	0.00
47	82-51	357.000	Till	clay	B.Spruce	1	1750	0.85	0.60	0.24	1.45	2.00	-4.7	-0.14	F	F	1	6.75
48	82-50	357.000	Till	silt/clay	Pine	1	1750	0.50	0.80	0.35	1.52	1.68	-4.7	0.29	U	F	0	0.00
49	81-1	357.000	Till	clay/sand	B.Spruce	1	1750	0.85	0.60	0.24	1.45	2.00	-4.7	-0.14	F	F	1	6.75
50	82-94	362.593	Till	clay	Pine	1	1750	0.50	0.80	0.35	1.52	1.68	-4.7	0.30	U	U	1	0.00
51	82-95	363.445	Till	silt/clay	W.Spruce	1	1750	0.80	0.80	0.31	1.41	1.90	-4.7	0.02	U	U	1	0.00
52	82-96	363.906	Till	clay/gravel	W.Spruce	1	1750	0.80	0.80	0.31	1.41	1.90	-4.7	0.02	U	U	1	0.00
53	82-97	367.242	Till	clay	B.Spruce	1	1750	0.85	0.60	0.24	1.45	2.00	-4.7	-0.12	F	F	1	6.06
54	82-98	368.754	Till	clay	B.Spruce	1	1750	0.85	0.60	0.24	1.45	2.00	-4.7	-0.12	F	F	1	5.95
55	82-99	368.754	Till	silt	Poplar	1	1750	0.55	0.90	0.30	1.59	1.82	-4.7	1.27	U	F	0	0.00
56	82-s42b	374.029	Till	sand/clay	Spruce	1	1750	0.80	0.80	0.31	1.41	1.90	-4.6	0.05	U	U	1	0.00
57	82-100	376.657	Till	sand	Spruce	2	1750	0.80	0.80	0.31	1.92	2.63	-4.6	-0.02	F	F	1	1.06
58	81-s42d	378.398	Till	clay	Poplar	1	1750	0.55	0.90	0.30	1.59	1.82	-4.6	1.29	U	U	1	0.00
59	82-101	381.465	Glaciofluvial	sand	W.Birch	2	1550	0.70	0.80	0.35	1.60	2.22	-4.6	-0.45	F	U	0	24.72
60	82-102	381.465	Glaciofluvial	sand	W.Spruce	2	1550	0.80	0.80	0.31	1.66	2.50	-4.6	-0.29	F	F	1	18.09
61	82-103	381.465	Glaciofluvial	silt/sand	Spruce	1	1550	0.80	0.80	0.31	1.26	1.84	-4.6	-0.21	F	F	1	9.47
62	82-104	385.433	Till	sand/clay	B.Spruce	2	1750	0.85	0.60	0.24	1.95	2.77	-4.6	-0.16	F	U	0	10.90

Record #	Borehole	KP	Terrain	Soil	Vegetation	Texture	Dry Density	Saturation (%)	Nt	Nf	Kt	Kf	MAAT	T_TOP	Predicted	Observed	Mode	Predicted Depth
63	81-3	389.926	Till	silt/gravel	B.Spruce	1	1750	0.85	0.60	0.24	1.45	2.00	-4.6	-0.09	F	F	1	4.52
64	82-83	392.848	Till	sand/clay	B.Spruce	2	1750	0.85	0.60	0.24	1.95	2.77	-4.6	-0.15	F	F	1	10.21
65	82-84	392.848	Lacustrine	clay	W.Spruce	1	1500	0.80	0.80	0.31	1.22	1.83	-4.6	-0.25	F	F	1	11.30
66	82-85	399.854	Till	clay	W.Spruce	1	1750	0.80	0.80	0.31	1.41	1.90	-4.5	0.11	U	F	0	0.00
67	82-86	399.854	Till	clay	B.Spruce	1	1750	0.85	0.60	0.24	1.45	2.00	-4.5	-0.08	F	F	1	3.85
68	82-87	401.587	Till	clay	B.Spruce	1	1750	0.85	0.60	0.24	1.45	2.00	-4.5	-0.07	F	F	1	3.73
69	81-4	407.268	Lacustrine	sand/clay	B.Spruce	2	1500	0.85	0.60	0.24	1.63	2.61	-4.5	-0.38	F	F	1	25.11
70	82-73	423.313	Till	clay	B.Spruce	1	1750	0.85	0.60	0.24	1.45	2.00	-4.4	-0.05	F	F	1	2.26
71	81-5	423.313	Till	sand	Birch	2	1750	0.70	0.80	0.35	1.85	2.34	-4.4	-0.07	F	F	1	3.81
72	82-74	426.281	Till	clay	Spruce	1	1750	0.80	0.80	0.31	1.41	1.90	-4.4	0.18	U	F	0	0.00
73	82-78	438.092	Till	clay	W.Spruce	1	1750	0.80	0.80	0.31	1.41	1.90	-4.4	0.20	U	F	0	0.00
74	82-77	439.331	Till	silt	B.Spruce	1	1750	0.85	0.60	0.24	1.45	2.00	-4.4	-0.02	F	F	1	1.18
75	82-76	439.331	Till	sand/silt	B.Spruce	2	1750	0.85	0.60	0.24	1.95	2.77	-4.4	-0.09	F	F	1	5.92
76	82-79	448.536	Lacustrine	clay	B.Spruce	1	1500	0.85	0.60	0.24	1.25	1.93	-4.3	-0.25	F	F	1	12.04
77	82-80	448.536	Lacustrine	clay	B.Spruce	1	1500	0.85	0.60	0.24	1.25	1.93	-4.3	-0.25	F	F	1	12.04
78	82-52	452.467	Lacustrine	silt/clay	B.Spruce	1	1500	0.85	0.60	0.24	1.25	1.93	-4.3	-0.24	F	F	1	11.80
79	82-53	454.528	Lacustrine	silt/clay	B.Spruce	1	1500	0.85	0.60	0.24	1.25	1.93	-4.3	-0.24	F	F	1	11.67
80	82-54	454.528	Till	clay	Poplar	1	1750	0.55	0.90	0.30	1.59	1.82	-4.3	1.48	U	F	0	0.00
81	82-55	462.349	Lacustrine	clay	B.Spruce	1	1500	0.85	0.60	0.24	1.25	1.93	-4.3	-0.23	F	F	1	11.19
82	82-56	464.817	Till	gravel/clay	B.Spruce	2	1750	0.85	0.60	0.24	1.95	2.77	-4.3	-0.05	F	U	0	3.57
83	81-9	470.088	Lacustrine	sand/clay	B.Spruce	2	1500	0.85	0.60	0.24	1.63	2.61	-4.2	-0.31	F	F	1	20.01
84	81-10	476.052	Aeolian	sand	Poplar	2	1600	0.55	0.90	0.30	1.54	1.82	-4.2	1.43	U	F	0	0.00
85	82-59	477.749	Aeolian	sand	Poplar	2	1600	0.55	0.90	0.30	1.54	1.82	-4.2	1.43	U	U	1	0.00
86	82-60	477.749	Aeolian	sand/clay	Pine	2	1600	0.50	0.80	0.35	1.49	1.68	-4.2	0.53	U	U	1	0.00
87	82-61	480.494	Lacustrine	sand/clay	Pine	2	1500	0.50	0.80	0.35	1.39	1.63	-4.2	0.36	U	U	1	0.00
88	82-63	485.676	Lacustrine	clay	B.Spruce	1	1500	0.85	0.60	0.24	1.25	1.93	-4.2	-0.20	F	F	1	9.76
89	82-62	485.676	Lacustrine	clay	B.Spruce	1	1500	0.85	0.60	0.24	1.25	1.93	-4.2	-0.20	F	U	0	9.76
90	81-b31a	494.123	Till	clay	W.Spruce	1	1750	0.80	0.80	0.31	1.41	1.90	-4.1	0.34	U	U	1	0.00
91	82-82	496.766	Organic	clay	Fen	3	300	1.00	0.70	0.12	0.52	1.70	-4.1	0.03	U	U	1	0.00
92	82-65	504.385	Glaciofluvial	clay/silt	B.Spruce	1	1550	0.85	0.60	0.24	1.29	1.94	-4.1	-0.13	F	F	1	6.40
93	82-66	507.996	Till	clay	Poplar	1	1750	0.55	0.90	0.30	1.59	1.82	-4.1	1.61	U	U	1	0.00
94	82-68	512.756	Glaciofluvial	sand/gravel	Alder	2	1550	0.70	0.85	0.30	1.60	2.22	-4.1	0.65	U	U	1	0.00
95	81-18	517.185	Organic	peat	Spruce Bog	3	300	1.00	0.50	0.14	0.52	1.70	-4.1	-0.50	F	F	1	21.18

Record #	Borehole	KP	Terrain	Soil	Vegetation	Texture	Dry Density	Saturation (%)	Nt	Nf	Kt	Kf	MAAT	T_TOP	Predicted	Observed	Mode	Predicted Depth
96	81-17	517.185	Organic	peat/clay	Spruce Bog	3	300	1.00	0.50	0.14	0.52	1.70	-4.1	-0.50	F	F	1	21.18
97	82-44	519.267	Till	clay/gravel	Poplar	1	1750	0.55	0.90	0.30	1.59	1.82	-4.0	1.64	U	U	1	0.00
98	81-s43a	527.256	Till	clay	Poplar	1	1750	0.55	0.90	0.30	1.59	1.82	-4.0	1.66	U	U	1	0.00
99	81-21	531.082	Aeolian	sand	Birch	2	1600	0.70	0.80	0.35	1.66	2.25	-4.0	-0.09	F	F	1	5.06
100	81-20	531.082	Lacustrine	sand	Alder	2	1500	0.70	0.85	0.30	1.54	2.19	-4.0	0.60	U	U	1	0.00
101	81-22	533.601	Aeolian	sand	Pine	2	1600	0.50	0.80	0.35	1.49	1.68	-4.0	0.66	U	U	1	0.00
102	82-1	535.493	Aeolian	sand	Pine	2	1600	0.50	0.80	0.35	1.49	1.68	-4.0	0.67	U	U	1	0.00
103	82-s1a	536.012	Colluvium	clay	Spruce	1	1440	0.80	0.80	0.31	1.18	1.81	-4.0	-0.08	F	F	1	3.59
104	82-s1b	537.478	Alluvial	silt/sand	Pine	1	1600	0.50	0.80	0.35	1.35	1.59	-4.0	0.49	U	U	1	0.00
105	82-13	538.902	Alluvial	silt	Spruce	1	1600	0.80	0.80	0.31	1.30	1.86	-4.0	0.19	U	U	1	0.00
106	82-s1c	540.184	Colluvium	sand/silt	Spruce	2	1440	0.80	0.80	0.31	1.53	2.44	-4.0	-0.17	F	F	1	10.57
107	81-23	544.362	Aeolian	sand	Poplar	2	1600	0.55	0.90	0.30	1.54	1.82	-3.9	1.60	U	U	1	0.00
108	81-24	545.473	Aeolian	sand	Pine	2	1600	0.50	0.80	0.35	1.49	1.68	-3.9	0.69	U	F	0	0.00
109	82-15	547.845	Aeolian	sand	Pine	2	1600	0.50	0.80	0.35	1.49	1.68	-3.9	0.70	U	U	1	0.00
110	81-25	550.489	Aeolian	sand	Spruce	2	1600	0.80	0.80	0.31	1.72	2.53	-3.9	0.10	U	F	0	0.00
111	81-26	550.489	Aeolian	sand	Pine	2	1600	0.50	0.80	0.35	1.49	1.68	-3.9	0.70	U	U	1	0.00
112	82-b2a	551.793	Aeolian	sand	Pine	2	1600	0.50	0.80	0.35	1.49	1.68	-3.9	0.71	U	U	1	0.00
113	82-18	556.212	Lacustrine	sand	Spruce-Poplar	2	1500	0.70	0.85	0.31	1.54	2.19	-3.9	0.53	U	U	1	0.00
114	81-27	556.675	Lacustrine	sand/clay	Spruce	2	1500	0.80	0.80	0.31	1.60	2.47	-3.9	-0.06	F	F	1	3.93
116	82-2	558.323	Lacustrine	sand	Spruce	2	1500	0.80	0.80	0.31	1.60	2.47	-3.9	-0.06	F	F	1	3.76
117	81-30	561.759	Organic	peat/clay	Fen	3	300	1.00	0.70	0.12	0.52	1.70	-3.9	0.17	U	U	1	0.00
118	82-20	565.044	Lacustrine	peat/clay	W.Spruce-Birch	1	1500	0.70	0.85	0.31	1.16	1.63	-3.9	0.61	U	U	1	0.00
119	82-19	565.044	Organic	clay	Fen	3	300	1.00	0.70	0.12	0.52	1.70	-3.9	0.18	U	U	1	0.00
120	81-33	574.754	Lacustrine	clay	Spruce-Poplar	1	1500	0.70	0.85	0.31	1.16	1.63	-3.8	0.63	U	F	0	0.00
121	82-s2a	576.703	Lacustrine	clay	W.Spruce	1	1500	0.80	0.80	0.31	1.22	1.83	-3.8	0.10	U	U	1	0.00
122	82-81	577.088	Organic	peat/sand	Fen	3	300	1.00	0.70	0.12	0.52	1.70	-3.8	0.21	U	U	1	0.00
123	81-34	580.853	Lacustrine	clay	B.Spruce	1	1500	0.85	0.60	0.24	1.25	1.93	-3.8	-0.08	F	U	0	3.93
124	82-5	580.853	Till	sand/clay	Pine	2	1750	0.50	0.80	0.35	1.67	1.76	-3.8	1.01	U	U	1	0.00
125	82-3	585.656	Till	sand/clay	Pine-W.Spruce	2	1750	0.50	0.80	0.35	1.67	1.76	-3.8	1.02	U	U	1	0.00
126	82-4	585.656	Till	clay	B.Spruce	1	1750	0.85	0.60	0.24	1.45	2.00	-3.8	0.24	U	U	1	0.00
127	82-6	595.785	Till	sand/clay	B.Spruce	2	1750	0.85	0.60	0.24	1.95	2.77	-3.7	0.17	U	F	0	0.00
128	82-7	595.785	Till	sand/clay	B.Spruce	2	1750	0.85	0.60	0.24	1.95	2.77	-3.7	0.17	U	U	1	0.00
129	82-8	596.833	Glaciofluvial	sand/clay	Spruce	2	1550	0.80	0.80	0.31	1.66	2.50	-3.7	0.11	U	U	1	0.00

Record #	Borehole	KP	Terrain	Soil	Vegetation	Texture	Dry Density	Saturation (%)	Nt	Nf	Kt	Kf	MAAT	T_TOP	Predicted	Observed	Mode	Predicted Depth
130	82-9	597.575	Till	sand/clay	Pine	2	1750	0.50	0.80	0.35	1.67	1.76	-3.7	1.05	U	U	1	0.00
131	82-10	597.575	Till	sand/clay	Pine	2	1750	0.50	0.80	0.35	1.67	1.76	-3.7	1.05	U	U	1	0.00
132	81-36	606.576	Organic	peat/clay	Spruce Bog	3	300	1.00	0.50	0.14	0.52	1.70	-3.7	-0.44	F	F	1	18.88
133	81-37	606.576	Organic	peat/clay	Spruce Bog	3	300	1.00	0.50	0.14	0.52	1.70	-3.7	-0.44	F	F	1	18.88
134	81-38	606.576	Organic	peat/clay	Spruce Bog	3	300	1.00	0.50	0.14	0.52	1.70	-3.7	-0.44	F	F	1	18.88
135	82-s3a	609.145	Colluvium	clay	W.Spruce	1	1440	0.80	0.80	0.31	1.18	1.81	-3.7	0.07	U	U	1	0.00
136	82-26	612.296	Till	clay	Spruce	1	1750	0.80	0.80	0.31	1.41	1.90	-3.7	0.63	U	U	1	0.00
137	82-29	616.895	Till	sand	Spruce	2	1750	0.80	0.80	0.31	1.92	2.63	-3.6	0.57	U	U	1	0.00
138	82-30	620.139	Till	gravel	Spruce	2	1750	0.80	0.80	0.31	1.92	2.63	-3.6	0.57	U	U	1	0.00
139	82-31	620.139	Till	clay	Pine-Poplar	1	1750	0.50	0.80	0.35	1.52	1.68	-3.6	0.91	U	U	1	0.00
140	82-s4a	632.612	Alluvial	sand/clay	Spruce	2	1600	0.80	0.80	0.31	1.72	2.53	-3.6	0.31	U	U	1	0.00
141	82-36	641.084	Till	clay	B.Spruce	1	1750	0.85	0.60	0.24	1.45	2.00	-3.5	0.34	U	U	1	0.00
142	81-39	646.537	Till	silt	B.Spruce	1	1750	0.85	0.60	0.24	1.45	2.00	-3.5	0.35	U	U	1	0.00
143	81-40	648.037	Organic	peat/silt	Spruce Bog	3	300	1.00	0.50	0.14	0.52	1.70	-3.5	-0.42	F	U	0	17.81
144	81-41	648.037	Organic	peat/silt	Spruce Bog	3	300	1.00	0.50	0.14	0.52	1.70	-3.5	-0.42	F	F	1	17.81
145	81-42	648.037	Till	clay	B.Spruce	1	1750	0.85	0.60	0.24	1.45	2.00	-3.5	0.36	U	U	1	0.00
146	82-37	652.496	Organic	silt	Fen	3	300	1.00	0.70	0.12	0.52	1.70	-3.5	0.37	U	U	1	0.00
147	82-b6a	657.657	Till	clay	Spruce-Pine	1	1750	0.70	0.80	0.31	1.34	1.70	-3.5	0.96	U	U	1	0.00
148	82-38	660.904	Till	silt/clay	B.Spruce	1	1750	0.85	0.60	0.24	1.45	2.00	-3.5	0.38	U	U	1	0.00
149	82-39	663.813	Till	sand	B.Spruce	2	1750	0.85	0.60	0.24	1.95	2.77	-3.4	0.30	U	U	1	0.00
150	82-b7a	669.619	Till	clay	B.Spruce	1	1750	0.85	0.60	0.24	1.45	2.00	-3.4	0.40	U	U	1	0.00
151	82-42	669.619	Till	clay/silt	B.Spruce	1	1750	0.85	0.60	0.24	1.45	2.00	-3.4	0.40	U	U	1	0.00
152	82-43	671.799	Till	sand/silt	B.Spruce	2	1750	0.85	0.60	0.24	1.95	2.77	-3.4	0.32	U	U	1	0.00
153	82-32	688.129	Till	clay	Pine	1	1750	0.50	0.80	0.35	1.52	1.68	-3.3	1.07	U	U	1	0.00
154	82-33	688.129	Till	gravel/clay	Spruce-Pine	2	1750	0.70	0.80	0.31	1.85	2.34	-3.3	1.04	U	U	1	0.00
155	82-24	695.938	Till	clay	Pine-Spruce	1	1750	0.50	0.80	0.35	1.52	1.68	-3.3	1.09	U	U	1	0.00
														Total Correct			**134**	
														% Correct			**87**	

APPENDIX 3
24 Off-ROW deep borehole data

Record #	Borehole	As-built Km	Terrain	Soil	Vegetation	Texture	Dry Density	Saturation (%)	Nt	Nf	Kt	Kf	MAAT	T_TOP	Predicted	Interpreted from T° logs	Code	Remarks
1	84-1	0.020	Lacustrine	clay/silt	Open b. spruce	1	1500	0.85	0.60	0.24	1.25	1.95	-6.2	-0.84	40.94	55	1	
2	84-2A	18.972	Till	clay/silt	B. spruce	1	1750	0.80	0.55	0.24	1.41	1.92	-6.1	-0.72	34.47	33	1	
3	84-2B	19.266	Colluvium	clay/shale	W. spruce	1	1440	0.80	0.80	0.31	1.18	1.84	-5.5	-0.65	29.66	30	1	Shallow bedrock (2m) - east-facing slope
4	84-2C	19.551	Colluvium	clay/silt	B. spruce	1	1440	0.80	0.55	0.24	1.18	1.84	-6.3	-1.03	47.08	53	1	Shallow bedrock (6m) -west-facing slope
5	84-3A	79.180	Lacustrine	silt/clay	B. spruce	1	1500	0.80	0.55	0.24	1.22	1.85	-6.1	-0.92	42.48	74	1	Cable T3 - north-facing slope
6	84-3B	79.395	Alluvial	sand/clay	B. spruce	2	1600	0.80	0.55	0.24	1.72	2.53	-6.0	-0.84	53.34	57	1	Top of north-facing slope
7	85-7A	271.231	Lacustrine	clay	Open b. spruce	1	1500	0.85	0.60	0.24	1.25	1.95	-5.1	-0.50	24.23	40	1	
8	85-7B	271.986	Lacustrine	clay	Open b. spruce	1	1500	0.85	0.60	0.24	1.25	1.95	-5.6	-0.71	34.48	70	1	Top of steep north-facing slope
9	85-7C	272.311	Lacustrine	clay/sand	Open b. spruce	1	1500	0.85	0.60	0.24	1.25	1.95	-5.1	-0.49	24.16	50	1	
10	84-4A	477.988	Aeolian	sand/clay	Pine	2	1500	0.50	0.80	0.35	1.39	1.63	-4.2	0.36	0.00		1	High water table
11	84-4B	478.116	Aeolian	sand	Pine	2	1500	0.50	0.80	0.35	1.39	1.63	-4.2	0.36	0.00		1	Dry surface - deep water table
12	85-8A	557.828	Lacustrine	sand/clay	W. spruce	2	1500	0.80	0.85	0.33	1.60	2.47	-3.9	-0.07	4.41	12	1	
13	85-8B	558.158	Lacustrine	silt/clay	Birch	1	1500	0.65	0.80	0.35	1.12	1.54	-3.9	-0.08	3.22	3.5	1	
14	85-8C	558.333	Lacustrine	clay	Birch	1	1500	0.65	0.80	0.35	1.12	1.54	-3.9	-0.08	3.21	3.5	1	
15	85-9	583.339	Till	granular	Open b. spruce	2	1750	0.85	0.60	0.24	1.95	2.77	-3.8	0.15	0.00		1	
16	85-10A	588.276	Till	clay/bedrock	Open b. spruce	1	1750	0.85	0.60	0.24	1.45	2.02	-3.8	0.22	0.00		1	
17	85-10B	588.686	Till	clay	Open b. spruce	1	1750	0.95	0.55	0.24	1.51	2.22	-3.8	-0.16	8.85	2	1	
18	85-11	597.396	Till	silt/clay	Open b. spruce	1	1750	0.85	0.60	0.24	1.45	2.02	-3.7	0.24	0.00	4	0	
19	85-12A	608.562	Till	clay	Open b. spruce	1	1750	0.85	0.60	0.24	1.45	2.02	-3.7	0.26	0.00		1	
20	85-12B	608.715	Till	peat/clay/gravel	Open b. spruce	1	1750	0.95	0.55	0.24	1.51	2.22	-3.7	-0.13	7.47	4	1	Frozen side of thermokarst interface
21	85-13A	682.233	Till	peat/clay	Open b. spruce	1	1750	0.95	0.55	0.24	1.51	2.22	-3.4	-0.04	2.41	3.5	1	
22	85-13B	682.422	Till	peat/clay	Open b. spruce	1	1750	0.95	0.55	0.24	1.51	2.22	-3.4	-0.04	2.40	7	1	
23	85-13C	682.633	Organic	peat/clay	Fen	3	300	1.00	0.70	0.12	0.52	1.70	-3.4	0.44	0.00		1	
24	84-5A	782.963	Organic	peat/clay	Bog	3	300	1.00	0.50	0.14	0.52	1.70	-2.9	-0.34	14.35	17	1	Peat plateau (4m peat)
25	84-5B	783.253	Organic	peat/clay	Bog	3	300	1.00	0.50	0.14	0.52	1.70	-2.9	-0.34	14.34	14	1	Peat plateau (6m peat)
26	84-6	819.508	Organic	peat/clay	Bog	3	300	1.00	0.50	0.14	0.52	1.70	-2.8	-0.32	13.41	9	1	Peat plateau (5m peat)
														Total correct			**25**	